**UNIVERSITY OF NAPLES FEDERICO II**

Department of Biology

**PhD in Biology**

**XXXV cycle**

# *Identification of potential persistence mechanisms engaged by the pathogen Moraxella catarrhalis using human in vitro respiratory models*

Candidate
**Dr. Martina Canè**

Tutor
**Prof. Marcello Merola**

Doctoral school coordinator
**Prof. Sergio Esposito**

Co-Tutor
**Dr. Alfredo Pezzicoli**

2019 - 2023

*È molto meglio perdersi*
*sulla strada di un*
*viaggio impossibile che*
*non partire mai.*

*(G. Faletti)*

## Disclaimer

**Sponsorship**: This work was funded by GlaxoSmithKline Biologicals SA.

**Transparence statement**: Martina Canè is a PhD student at University of Naples Federico II and participates in a post graduate studentship program at GSK, Siena, Italy.

# Index

## Abstract

Moraxella catarrhalis (Mcat) is a Gram-negative diplococcus bacterium that colonizes the upper and lower respiratory tracts in human. Although it has long been considered a commensal bacterium, Mcat has been recognized as one of the causative agents of otitis media (OM) in children and exacerbation of chronic obstructive pulmonary disease (COPD) in adults where it forms polymicrobial communities with Nontypeable *Heamophilus Influenzae* (NTHi). The widespread resistance to β-lactam antibiotic treatments and the employment of undefined persistence mechanisms, along with the lack of suitable animal models to understand the etiology of infection make its eradication complicated and development of innovative *in vitro* alternatives urgent.

The human airway epithelium is the first line of defense against inhaled pathogens, acting as a physical, chemical, and immunological barrier. Modeling human-derived lung epithelial barrier *in vitro* could represent a valid tool for the characterization of host-pathogen interaction and shed light on *Moraxella catarrhalis* persistence systems. To that purpose highly physiological human-derived *in vitro* models has been assembled. Co-cultures of epithelial and stromal cells on porous transwell membrane allowed to obtain fully-differentiate human epithelial tissues displaying physiological features of *in vivo* lung tissue, such as the formation of a pseudostratified architecture composed of different cell types, and a functional epithelial barrier with an active mucociliary clearance system. In this context, we aimed to monitor Mcat infection progression to investigate pathogen-associated invasive and persistence strategies in the host environment.

At the early stages of infection, Mcat targeted preferentially epithelial ciliated cells and showed the ability to adapt to the new environment by modulating the expression of specific virulence factors. Interestingly, when the infection occurred in concomitance with NTH, the expression of genes involved in iron uptake and β-lactam antibiotic resistance were differently regulated respect to single-infected models suggesting the presence of mechanisms of transcriptional regulation that were active between the two pathogens. After the initial adaptation phase Mcat was

observed to actively invade the host epithelium by modulating the eukaryotic cytoskeleton for internalization inside cells. Interestingly, fluorescence and electron microscopy analysis revealed Mcat ability to subvert host clearance mechanisms and to replicate inside the cell cytosol giving rise to massive intracellular colonies that subsequently expanded by invading neighboring cells. Importantly, these dense biofilm-like structures appeared to form inside the epithelial layer and subsequently emerged to originate large surface-associated bacterial communities suggesting a colonization mechanism that relies on both intracellular and extracellular bacterial lifestyle. This aggressive invasion phenotype caused significant remodeling of the pseudostratified host tissue, especially at the level of luminal cells with activation of stimulatory mechanisms for tissue regeneration.

In conclusion, *in-house* assembled *in vitro* systems made it possible to identify potential invasive and persistence strategies used by Mcat in complex, self-sustaining airway infection context, creating the basis for the identification of bacterial antigens that could be used as candidates for new potential vaccines interventions.

# Introduction

## 1.1 The human respiratory mucosa

The respiratory apparatus is a complex organ system that is divided into two parts: the upper respiratory tract and the lower respiratory tract. The former includes the nasal cavity, pharynx, and larynx. The latter can be further divided in three zones according to the cellular phenotypes present: the proximal airway (trachea and bronchi), the bronchoalveolar duct junction and the alveoli[1]. Each area has a specific function that is reflected in the specialized cells covering the respiratory system from the nasal cavity to the alveoli [2]. In recent years, the use of advanced techniques has expanded our knowledge of cell sub-types composing the respiratory tract, discovering new cell categories and new cell functions[3].

Associated to the basal membrane the cuboidal basal cells represent the principal source for airway epithelial renewal, acting as stem cells of the respiratory system. Indeed, these cells have a critical role in regulating respiratory homeostasis and, more importantly, epithelium regeneration post-injury[4]. Notably, one of the first respiratory abnormalities observable in both heavy smokers and COPD patients is the basal cell hyperplasia, highlighting a key role for these cells in disease development [5]. Columnar ciliated cells completely cover the airways, thus playing a key role in capturing and expelling mucus, pathogens and debris through the rhythmic movement of the cilia, commonly called muco-ciliary clearance mechanism (MMC) [6]. This function is exerted in cooperation with the goblet cells whose primary role is the production of mucus, a substance essentially composed of electrolytes, metabolites, fluids, antimicrobial products, and mucins. However, excessive mucus production is a symptom associated with several lung diseases such as COPD, asthma, and CF [7]. Other secretory cells are mainly localized in bronchioles and include club cells (or Clara cells). They produce uteroglobin, an amphiphilic surfactant layer whose function is to reduce surface tension and that has anti-inflammatory and immunosuppressive action. In addition, Club cells retain stem cell properties, since they are able to generate ciliated and club cells or, in some conditions, even to dedifferentiate into basal cells. These cells play an important role in regulating airways homeostasis, and their alteration is a condition

that strongly contributes to the dysregulation observed in common respiratory diseases (COPD, CF, Asthma) [7]. Amongst other cell types, the tracheobronchial epithelium also includes Tuft cells which are microvillous cells believed to have chemosensory, neuronal and immunological functions. In proximal airways also pneumoendocrine cells can be detected (PNEC). They constitute the 5% of the entire epithelial population, and they serve as a communication bridge between the immunological and nervous systems. Among the newly discovered cells subsets, there are ionocytes, which represent approximately 2% of respiratory epithelial cells [8], and hillock cells whose function is still unknown[9].

The structure and the cellular composition of the epithelium progressively vary with the degree of branching, switching from pseudostratified to cuboidal in the small bronchi and bronchioles, with the reduction of ciliated cells and predominance of secretory Club cells. In the distal alveolar region of the lung, two different types of cells that are phenotypically and functionally distinct are present: a) the alveolar epithelial type 1 (AT1) cells specialized in gas exchange; b) type 2 cells (AT2) producing pulmonary surfactant substance that is responsible for the protection against inhaled irritants[10]. Increased mucus production by goblet cells is a common feature of asthma, COPD, PCD, and CF pathologies (Fig.1).

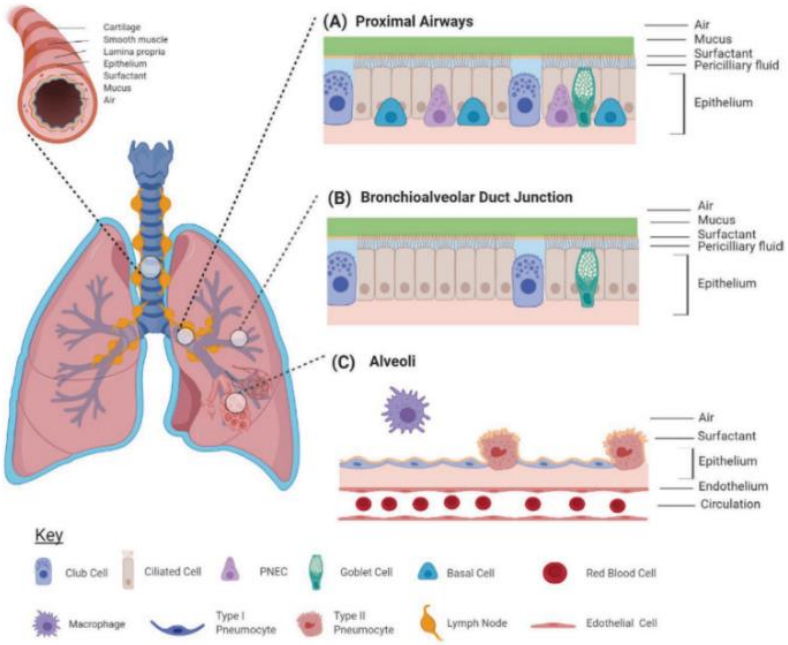


***Figure 1**. Schematic representation of the human respiratory tract. (Barron et al. 2020).*

## 1.2 Immunity in the respiratory mucosa

The respiratory epithelium is constantly exposed to inhaled environmental particles, pollutants, allergens, and microbes. For this reason, airways are endowed of wide variety of cellular and humoral host defense mechanisms that allow to maintain epithelial barrier integrity and lung homeostasis, with disruption leading to the development of inflammation and disease[11]. The primary defense mechanism is represented by its proper morphology which create an effective physical barrier against the environment. In addition, respiratory cells secrete a wide variety of effectors which directly bind to and inactivate infectious agents. Furthermore, epithelial cells display a range of specialized receptors capable of sampling the airway lumen for non-harmful, immunogenic, or pathogen derived antigens[12]. The activation of these unique Pattern-Recognition Receptors (PRRs) triggers a variety of immunogenic and pathogen-clearing pathways, including the early inflammatory response, the recruitment of innate immune cells, and the activation of the adaptive immune response[10].

### 1.2.1 The physical barrier

The respiratory epithelium of the upper airways forms the first physical, chemical and immunological barrier that protects the body against external aggressions such as allergenic, pathogenic microorganisms and inhaled irritants [13]. To exploit the function of the physical barrier, lung epithelial cells are oriented along an apical-basolateral polarity axis. This polarity is ensured by key elements that separate the apical and basolateral compartments of plasma membranes which form the apical junctional complex (AJC) composed by tight junctions (TJ), adherens (or anchoring) junctions (AJ) and gap junctions that exploit their organization and function coordinately [14].

TJs main functions are to ensure the non-permeability of the epithelium to external elements, along with the regulation of paracellular ionic movements. They are composed of most known claudins and occludins, and the framework forming proteins multi-PDZ domain protein 1 (MUPP1), proteins associated with lin even 1 (Pals1), and zonula occludens (ZO1, ZO-2, ZO-3) which connect transmembrane

proteins with actin cytoskeleton. The functionality of the TJs is determined by the interaction of the transmembrane claudins with the corresponding protein located on neighboring cells. The interaction of the intracellular carboxyterminal domain with the scaffold protein ZO-1 ensures the anchorage to cellular cytoskeleton[15] (Fig.2). Below the TJ, AJs and desmosomes are involved in cell-to-cell basolateral interaction. The AJ transmembrane protein, E-cadherin interacts with α/β-catenin mediating the interaction with cytoskeleton components, thus exploiting a pivotal function in cellular pathways signaling and gene expression [13]. Additionally, desmosomal proteins provide many epithelial tissues the ability to resist to mechanical stress. They mediate the interaction between the transmembrane proteins of adjacent cells and the desmosomal plaques, which recruit intermediate filament components, such as the keratins[16]. Keratins, apart from providing mechanical stability and integrity to epithelial cells, exert important regulatory function and mediate intracellular pathways related to apoptosis, wound healing and stress protection[17]. Finally, the main function of gap junctions is to guarantee cell-to-cell communication by forming channels that connect the cytoplasm of each cell and allow molecules, ions, and electrical signals to flow among them.

Increasing knowledge on structures and functions of TJ proteins has revealed their essential role in establishing cell polarity of tissue layer, as well as regulation of cellular functions such as proliferation, differentiation, and migration by recruitment of signaling proteins[18]. TJs assembly and disruption are controlled by kinases of the Ras homolog (Rho) GTPase/Rho Kinases (ROCK) pathway. It can regulate TJ stability by the ratcheting of actin and myosin [19]. Inadequate mucosal barriers in gut, skin and lower airways are strictly linked to the onset of chronic inflammatory disease; indeed, the increased permeability of the epithelium may contribute to the chronic stimulation of the immune system and to downstream inflammatory responses. Furthermore, certain bacteria and virus have evolved

mechanisms to disrupt the epithelial barrier and effectively infect and damage the epithelium [13,20].

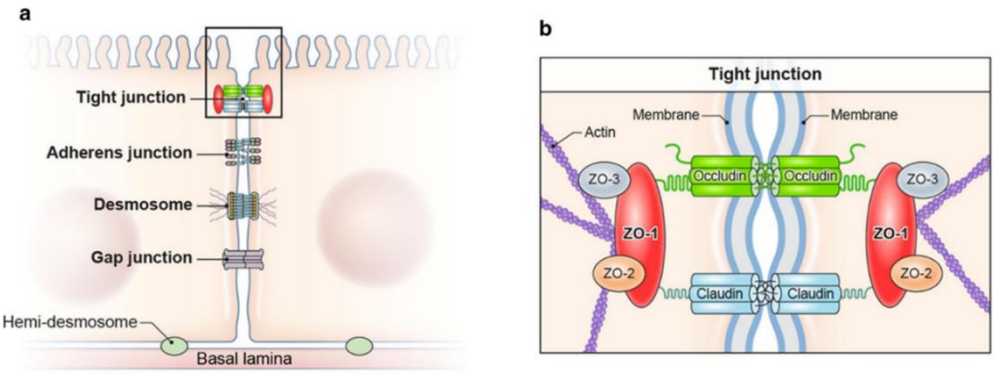


***Figure 2 a*** *Epithelial cell-cell junction scheme* ***b*** *Detailed view of protein–protein interactions between the tight junction and actin cytoskeleton* ***(J. M. Robinson* and W. A. Henderson. 2018)***

### 1.2.2 Mucociliary clearance and antimicrobial peptides

The proximal airways consist of an epithelial layer composed by basal, Club, goblet, and ciliated cells. These cells can produce several substances forming the surfactant, periciliary and mucus layers overlaying the epithelium. Mucus, released by goblet and submucosal glands, is composed by 97% of water, with a trace amount of lipids, proteins, and carbohydrates. The most prevalent proteins are mucins, which give to the mucus a gel-like consistency and negative charges. With the coordinated beating of cilia (mucociliary clearance), inhaled particles, poisons, and pathogens are removed from the respiratory tract [10]**.** In contact with cilia, there is the periciliary fluid layer which contains anti-fungal, anti-viral, and anti-microbials substances. Between the mucus and periciliary fluid, a surfactant amphiphilic substance secreted by Club cells (and alveolar type 2 pneumocytes in alveoli) is present. The surfactant, mainly composed by phospholipids and cholesterol reduces surface tension and increases respiratory compliance [10] (Fig. 1). In response to the production of inflammatory cytokines during infection, epithelial cells can release antimicrobial proteins and peptides (AMP). These charged peptides can bind to the bacterial surface, thus exerting antimicrobial functions on a wide variety of pathogens. Defensins, cathelicidins and LL37[21] belong to this group.

### 1.2.3 Pattern recognition receptors

Airway epithelial cells, alveolar macrophages, antigen presenting cells and neutrophils constitutively express a broad spectrum of Pathogen Recognition Receptors (PRRs) localized extracellularly and intracellularly to sense pathogens and activate immune response[22]. The PRRs can be both transmembrane and cytosolic receptors able to detect in different subcellular districts pathogen-associated molecular patterns (PAMPs) such as lipopeptides, nucleic acids, and bacterial proteins, prompting a fast and effective response to infection. Among them, we can find the transmembrane Toll-like receptors (TLRs), nuclear oligomerization domain (NOD), and retinoic acid inducible gene-I (RIG-I). The most widely expressed in the lung are the TLR. Several TLR are restricted to endosomes ad are activated if their ligands are delivered via endocytic/phagocytic pathways[23]. Once identified the threat, the lung epithelium can respond enhancing barrier defense with stimulation of mucociliary function, reinforcement of cellular junctions and modulation of cytoskeletal elements to exclude bacteria, triggering production of antimicrobial peptides to directly contrast the pathogen, or inducing cytokines production to recruit leukocytes.

### 1.2.4 Phagocytosis

The epithelium of mucosal tissues is continuously exposed to particles, pollutants, and microbes. It is not surprising that it has multiple mechanisms to sense potential danger and orchestrate pathogen clearance (mucus production, antimicrobial peptide production, muco-ciliary clearance, and phagocytosis) conducting the first steps of the immune response[24]. Moreover, epithelia secrete cytokines to recruit immune cells and potentiate their antimicrobial activities [21].

The host tolerates commensal bacteria or colonizing pathogens that are concentrated more in the upper respiratory tract to prevent unnecessary inflammatory damage[25]. Nonetheless, the epithelium possesses a variety of weapons to totally eradicate or severely restrict the growth of infections, such as phagocytosis which plays a central role in host defense. While professional phagocytes rely on recognition of Fc portion of IgG bound to pathogens for their

uptake and destruction, non-professional phagocytes as epithelial cells are able to perform a similar process but using different mechanisms [21,26]. These cells, indeed, do not express receptors for opsonic phagocytosis, rather it is quite common for bacteria themselves to initiate the phagocytosis mechanism: pathogens can modulate the actin cytoskeleton of host cell using so-called "zipper" or "trigger" mechanisms[26]. In "zipper" mechanism, bacterial surface adhesins interact with host membrane components (adhesin, integrins and cadherins) inducing actin/microtubule rearrangements at contact site resulting in bacteria internalization[26]. An example of such a mechanism is represented by *Listeria monocytogenes* invasion of intestinal epithelium. This bacterium expresses two surface proteins, InlA and InlB, which respectively target E-cadherin and the hepatocyte growth factor receptor Met. The interaction results in cytoskeleton remodeling at site of entry and bacterial internalization[27]. The "Trigger" mechanism involves the secretion of effectors into the host cell by the pathogen that cause large scale cytoskeleton rearrangement mediated by Rho family GTPase components. This process results in formation of membrane ruffles at point of contact that enfold the pathogen and, finally, vesicles sealing. The expansion of pseudopods is induced by the continuous assembly of actin filaments, which leads to the elongation of membranes. Soluble factors are usually injected via type III secretion systems, as observed for the enteric pathogen *Salmonella*. Some of the effectors activate Rho GTPases that spatiotemporally stimulate actin cytoskeleton rearrangements and allow membrane ruffling[28].

Although the process is initiated by the pathogen, the host is actively involved in its internalization and subsequent maturation of the resulting phagosome. After pathogen-induced internalization, the nascent phagosome undergoes a series of fusion and fission mechanism with endocytic organelles that enrich the membrane of the vesicles with proteins necessary for each stage of phagosome maturation (early, intermediate, late endosome and phagolysosome) such as Ras-associated binding GTPases, vacuolar ATPases, acid hydrolases, and acidic proteases. Rab 5 and Rab 7 GTPase coordinate the maturation process, while the progressive acidification of the lumen is mediated by the early recruitment of vacuolar ATPases.

The acquisition of membrane proteins associated with lysosomes 1 and 2 (LAMP-1 and LAMP-2) by the late endosome is fundamental to allow the fusion between late phagosomes and lysosomes. These organelles are distributed in the cytosol of mammalian cells and contain more than 60 acid hydrolases which require low pH to be activated such as glycosidases, DNAses, cathepsins, proteases, lysozymes, and lipases. Finally, phagolysosomes membranes are enriched with NADPH oxidase complexes (NOXs), which generate ROS, including superoxide anion (O2•−), hydrogen peroxide (H2O2) and hydroxyl radical (OH•). Therefore the mature lysosome creates a controlled and confined environment for killing and degradation of internalized pathogens.

In response to these human defensive mechanisms, many bacteria have evolved strategies to specifically escape these processes. Günther et al provides a wide and exhaustive review of the escape mechanisms used by bacteria to overcome the defense systems of epithelial barriers[26]. Pathogens can alter the protein and lipidic composition of endocytic vacuoles or modify their trafficking. Some of *Salmonella*' effectors, for example, can block ROS production occurring on phagolysosome preventing NADPH assembling and recruitment[29]. Alternatively, Listeria monocytogenes can produce a pore forming toxin which allows the pathogen to escape from the phagosome, replicate in the cytosol and invade adjacent cells[30]. Failure of bacterial degradation inside the lysosome, together with adaptations of the pathogen to the new cellular environment, could causes missed bacterial PAMPs recognition by the host. Although professional and non-professional phagocytic cells follow the same basic principles for phagocytosis, phagocytic killing is less efficient in epithelium cells as compared to phagocytes. Nonetheless, the large number of epithelial cells lining the respiratory tract are able to contribute considerably to pathogen clearance.

Despite pathogen escaping into the cytosol, the host is still able to recognize the pathogen and activate a specific autophagy mechanism, the xenophagy. Cytosolic bacteria are tagged by ubiquitin and cytosolic galectins that are usually localized within a vacuole. Subsequently, microtubule- associated protein light chain 3 (LC3)

mediates anchoring of bacterial-bound ubiquitin to the autophagosomal membrane. Finally, the autophagosome is delivered to lysosomal degradation. PAMP-activated TLR and NOD signaling enhances the speed and effectiveness of the process.

A new mechanism linking phagocytosis and autophagy has recently been discovered operating in professional and non-professional phagocytes. Using a not well-defined mechanism, the activation of vesicles-located sensors including PRRs induce the activation of LC3-mediated phagocytosis (LAP). Pathogen-containing vesicles are coated on the external leaf with (LC3) forming LAPosome that is rapidly delivered towards lysosome degradation[31].

Despite the wide variety of mechanisms employed by respiratory epithelia to counteract bacterial infection, pathogens have evolved complex and undefined strategies to manipulate the host immune defense and successfully colonize epithelial tissues.

### 1.2.5 Host cell death

The immune response to pathogens in lungs needs to be carefully regulated to prevent uncontrolled pathogen replication and lethal tissue destruction as results of microbial toxins or host inflammatory response[32]. Host PRRs detection of bacterial PAMP/DAMP activate downstream stimulation of bactericidal effectors functions such as the formation of reactive oxygen species (ROS), phagocytosis, or the secretion of mucus and bactericidal proteins in epithelial cells[33]. Pathogen-overloaded PAMP-sensing cells will also activate programmed cell death processes such as apoptosis, necrosis, pyroptosis[34–36] and cell exfoliation [35,36].

Cell death represents an intrinsic mechanism of immune defence employed by the host in response to the microbial infection. Sacrificing the infected cell represents a fundamental immune defence mechanism in multicellular organism to ensure the survival of adjacent healthy cells and to maintain tissue functionality[32,37]. Membrane blebbing, cell shrinkage, DNA fragmentation, mitochondrial permeability, and caspase activation are the morphological features of the

programmed cell death process called apoptosis[37,38]. Bacteria are retained within apoptotic bodies and ingested by phagocytic cells during apoptosis. This energy-dependent, irreversible and highly coordinated program leads to the ordinated disassembly of dying cells without any release of the cytoplasm content, or the organelles and nucleus, into the extracellular space. This approach allows both to prevent the emission of an alarm signal at early stage of infection but also induce engulfment of apoptotic bodies by phagocytic cells inducing a protective immune response[39]. Instead, the pro-inflammatory cell death necrosis is characterized by membrane rupture, nuclear enlargement, release of cellular contents, and inflammation not-related to caspase activation. ROS production or danger signals (lysosomal destabilization, calpain release, and depletion of ATP) induced upon bacterial infection trigger the necrosis pathway[37,40]. In pyroptosis, the PAMP/DAMP recognition induce the inflammasome assembling which mediate caspase 1 and pyroptosis activation. The pyroptotic cell undergoes to membrane rupture, DNA fragmentation, and the release of pro-inflammatory cytokines, including IL-1β and IL-18[41,42].

Nevertheless, many pathogens have evolved strategies to manipulate the host response during infection to promote bacterial survival[43,44]. Using a wide variety of mechanisms, intracellular bacteria generally try to create an intracellular safe niche for replication inhibiting apoptotic signal transduction. As an example, it is reported the ability of some intracellular bacteria like *Legionella pneumophila*, *Chlamydia trachomatis* or *Mycobacterium tuberculosis* to produce and secrete factors able to interact and then inhibit or degrade pro-apoptotic factors in the host cell[45–47]. On the other hand, some intracellular bacteria such as *L. pneumophila* can activate host anti-apoptotic signalling regulated by the innate immune response master regulator NFkβ[48,49]. Other pathogens have developed elaborate strategies to ensure successful infections such as *M. tuberculosis* that uses two distinctive strategies during macrophage infection to control cell death. At the early stages of infection this pathogen upregulates TLR2/NFkβ signalling to delay apoptosis progression, and secretes factors that inhibit ROS generation in the phagolysosome. At later stages of infection, *M. tubercolosis* increases macrophages apoptotic rate to facilitate the

egress of intracellular bacteria and further infection of other cells [50,51]. Similarly, enteropathogenic *E. coli* (EPEC) delivers a subset of effectors into the intestinal epithelium manipulating a variety of host signalling pathways such as cytoskeletal rearrangement, disruption of cell–cell junctions, epithelial cell death, and immune modulation[52]. Within the great diversity of strategies employed by respiratory bacteria we can roughly divide them in two groups. The pro-inflammatory pathogens take advantage from the necrosis and immune response-related tissue damages to cross the epithelial barrier and colonize other organs. The second group rely on the suppression of bacterial detection mechanisms and on the upregulation of host factors that promote survival and replication of the pathogen. These pathogens tend to create a stable niche for replication and for the establishment of chronic infection[32].

### 1.2.6 Epithelial cell extrusion

Cell extrusion is a mechanism commonly used by epithelia to remove damaged and dying cells while preserving its function as protective barrier. Epithelia are regularly subjected to turn over between dead and newborn cells, maintaining an homeostatic cell number [53]. The dying cells extrudes the lipid Sphingosine 1 Phosphate (S1P), which binds to the G-protein-coupled receptor Sphingosine 1 Phosphate receptor 2 (S1P2) in the surrounding cells and stimulates Rho-mediated contraction of an actomyosin ring basally and circumferentially. The aim of this contraction, in response to apoptotic, crowding- or infection induced stimuli [54], is to force the cell out of the epithelial barrier while maintaining intact the epithelial barrier. Importantly, extrusion is an essential mechanism of host defense against microbes because it prevents or at least minimize their passage through the epithelial barriers. Consequently, a dysfunctional cell extrusion process can negatively affect the integrity of the barrier promoting the onset of inflammatory processes and invasion of pathogens [54].

Nevertheless, many bacteria have evolved mechanisms to exploit cell extrusion to infect host tissues. For instance, *Listeria monocytogenes* takes advantage of the extruding cells mechanism to gain access to host proteins that are not commonly

exposed to the luminal side of the gut and that became exposed during the extrusion process [55]. Furthermore, excessive extrusion of infected cells can result in their accumulation in the intralumenal region, causing inflammation and airway obstruction, as observed during RSV infections [56]. Conversely, some pathogens have developed strategies to prevent the extrusion mechanism by acting on the attachment of the cell to basal membrane. For example, it has been reported that *Neisseria gonorrhoeae* through the binding of the colony opacity-associated (Opa) proteins to human carcinoembryonic antigen-related cell adhesion molecules (CEACAMs) is able to enhance the expression of CD105 receptor (member of TGF-β1 receptor family)[57]. This receptor binds to β1-integrin, via its association with Zyxin and ZRP-1, reinforcing the adherence of the infected epithelial cells to the ECM. It is interesting to speculate that other human-specific bacterial pathogens interacting with CEACAM such as *Heamophilus influenzae* and *Moraxella catarrhalis* could employ a similar mechanism [57].

### 1.3 Modeling the tracheo-bronchial mucosa *in vitro*

In recent years, there has been a growing interest in the development of *in vitro* systems to study respiratory diseases. So far, the animal model has been widely used for toxicology application[58]. However, considerable difficulties have been encountered in animal-human translation due to the significant anatomical and physiological differences existing. Human respiratory disorders including asthma, chronic obstructive pulmonary disease (COPD), and pulmonary fibrosis in animal models are not completely equivalent to human diseases, which results in high failure rates of clinical trials in animal[59]. Therefore, the principle of Reduction, Replacement and Refinement of 3R project proposed by Russel and Burch, outlined the need for the scientific community to develop more physiologic *in vitro* models to replace the use of animals in testing [60].

These systems are based on cell culturing in laboratory with the final issue to recreate structural, morphological, and functional surrogate of specific human regions. Culturing of 2D homotypic submerged monolayer derived from human respiratory tissue has been widely used as an instrument for respiratory and

toxicology research *in vitro*[61]. Although it represents a simplified system for the evaluation of basic cellular responses, this model does not adequately represent the differentiated phenotype of the airway epithelial tissue *in vivo*. The increasing demand for more reliable and predictive models enhanced the efforts made to recreate the lung architecture to mimic tissue microenvironment, a topic extensively discussed in a large number of reviews ([10,58,60,62,63]). Many *in vitro* systems that mimic the natural lung environment have been developed as a result of improvements in tissue-engineering tools and cell-culture procedures. The selection and design of a complex *in vitro* system goes through the evaluation of different factors such as the cells source (immortalized, primary cells), their anatomical region of origin (proximal and distal epithelium, immune cells), mono-cultured or co-cultured cells, the scaffold, and the extracellular matrices or hydrogels that should resemble tissue microenvironments and architectures. Currently developed respiratory airway models are Air-liquid interface (ALI) cultured tissues, organoids and, organ-on-chip.

Developed in the late 1980s, organotypic ALI models are made up of a chamber with a semipermeable support which separates the culture environment in two compartments: the basal side, where culture medium is supplied through the membrane and the apical chamber where the exposition of cells to the surrounding air promotes cellular differentiation[64] and function. Under these stimuli, primary airway cells derived from different lung regions (nasal, proximal, distal) are differentiated into an heterogenous cell population with polarized mucociliary phenotypes [65] in which metabolic function, barrier properties, and in-vivo-like transcriptional profiles resembles organotypic features[60]. The peculiar configuration of the transwell system enabled the integration of more cell types, depicting the rich cellular population forming the pulmonary environment (e.g. epithelium, dendritic cells, fibroblasts, endothelium) [66]. The ALI model permits to recreate a differentiated organotypic system that reproduce many of the *in vivo* features such as the formation of a physical barrier, physiological systems such as the mucociliary clearance, and reproduce an *in vivo*–like transcriptional profile[67]. Consequently, because of their physiological similarity to *in vivo* airway epithelia,

primary cell-based ALI tissue cultures have been used as *in vitro* models to deconstruct intricate pathophysiological processes such as acute epithelial injury, fibrosis, COPD, asthma, and cancer, as well as pathogenesis of respiratory pathogens[66].

### 1.4 Infection of the respiratory tract

Although it has been considered a sterile environment for a long time, new sequencing techniques have made possible to identify the presence of a wide variety of microbes colonizing healthy lungs over their entire length[68]. Genetics factors and lifestyle habits such as smoking, alcohol consumption and physical activity strongly influence the composition and diversity of lung microbiota during lifetime[69]. Indeed, alteration in microbial composition (dysbiosis), compared to healthy subjects, has been observed in patients with cystic fibrosis (CF), chronic inflammatory diseases, asthma, and allergy[70,71]. The most common bacteria colonizing different tracts of the respiratory system belong to *Dolosigranulum, Moraxella, Prevotella, Veillonella, Corynebacterium, and Staphylococcus* genera; the balance between these species acts as gatekeeper of human health by preventing the colonization of bacterial pathogens[72].

Increasing evidence shows that the severity and clinical outcome of COPD is strongly associated to the structure and diversity of the lung microbial community[73]. In addition, microbiome analysis of subjects affected by mild-to-moderate COPD exhibited a decrease of *Prevotella* abundance and an increase in the presence of *Moraxella* genera related to an worsening of symptoms[74]. Furthermore, a longitudinal epidemiological Acute Exacerbation and Respiratory infectionS study in COPD (AERIS) subjects assessed that the incidence and severity of AECOPD during the exacerbation are related to an increased bacterial load, with the enrichment of potentially pathogenic bacteria such as *Heamophilus influenzae, Streptococcus pneumoniae and Moraxella catarrhalis*[75]. Additionally, the higher bacterial load of these pathogens correlated with more severe airflow limitation in stable COPD[76].

### 1.4.1 *Moraxella Catarrhalis*

*Moraxella catarrhalis (Mcat)* is a Gram-negative diplococcus that commonly colonizes the mucous membranes of the human nasopharynx. *Moraxella* species are normally aerobic, uncapsulated, and non-motile. Although, it has long been considered a commensal bacterium, Mcat has been recognized as one of the top three most frequent etiologic causes of respiratory tract diseases[77]. It mainly forms polymicrobial communities with *Streptococcus pneuomonie* and *Heamophilus Influenzae*. Moreover, it is associated with laryngitis, bronchitis and pneumonia[78] along with being a causative agent of otitis media in children and exacerbation of COPD in lower tract of adults[79].

To date, the main approach to treat pathogen-related diseases involves the use of antibiotics; however, approximately 95– 99% of clinical isolates screened are able to produce beta-lactamase enzyme, which reduces the spectrum of possible antibiotic treatment to non-beta lactams[80]. The constant spread of antibiotic resistance is pushing for the development of alternative method to treat the still not well-understood *Moraxella* mechanism of infection; therefore, its understanding would be essential for the identification and formulation of effective vaccines.

#### 1.4.1.1 Mcat virulence factors

In order to establish a successful colonization and infection of the middle ear, oropharynx and bronchial surfaces of lung, *Moraxella* expresses a huge variety of surface adhesive molecules that juxtaposed to epithelial receptors, extracellular matrix, and inflammatory mediators of the host (Fig.3). The urging to formulate an effective vaccine against Mcat infections has prompted research towards antigens identification and evaluation as valid vaccine candidates, which are continuously and extensively reviewed[81–83].

Adherence to the respiratory mucosa is an important step in the process of bacterial colonization and infection of the respiratory tract epithelium. Mcat adherence factors include fimbriae, type IV pili, fimbrial-unrelated adhesins and non-protein components. Fimbrial factors, also termed as pili or fibrils are surface

heteromeric, multi-subunit protein complexes, with only a minor component which properly works as adhesin, by interacting with glycan moieties found in glycoproteins and glycolipids of host organisms. Human ganglioside M2 is the receptor for PilA, the pilin subunit of type IV Mcat pilus[84], protein that contribute to the long range adhesion of the bacterium [85]. Mcat adherence protein (McaP), outer protein CD (OmpCD), Mcat filamentous Hag (FHA)-like proteins (Mha proteins), Mcat immunoglobulin D (IgD) binding protein/hemagglutein (MID/ Hag), and ubiquitous surface proteins (Usps) belong to non-fimbriae type adhesins [77].

Despite their tight integration into the bacterial outer membrane, trimeric autotransporter adhesins (TAA) are involved in long distance interaction as well. They are equipped with a coiled-coil domain that elongates the amino-terminal head domain away from bacterial surface allowing the interaction with components of the host surface. To this class belongs the ubiquitous surface proteins family, which consists of UspA1, UspA2 and hybrid UspAH proteins. UspA1 binds carcinoembryonic antigen-related cell adhesion molecule 1 (CEACAM1) [86], causing suppression of human inflammatory response [87], and along with UspA2, it interacts with ECM proteins as laminin, fibronectin, and vitronectin[88] that contribute to pathogen serum resistance [89,90] and other virulence mechanisms. UspA1 and UspA2 are surface-exposed antigens and that are antigenically conserved among the clinical isolates [91] which rendered them promising vaccine candidates in the past. However, DNA analyses conducted on several Mcat isolates revealed the presence of numerous repeated sequences corresponding to the loci of the *UspA1*, *UspA2/AH*, *mid/hag*, and cytoplasmic localized Type III DNA methyltransferases (*modM* and *modN)* genes[81]. The exchange of the peptide sequence “cassette" mediates the change in gene expression resulting in a highly mutable genome. Consequently, phase variation contributes to increase the virulence of the pathogen enabling it to easily adapt to the host environment and conferring differing phenotypes among several Mcat isolates [92]. This mechanism made even more challenging the identification of a valid, stable expressed vaccine candidate. Recently, because of its cross-reactivity, UspA2 antigen is capable of

inducing a cross-protective antibody response against a wide range of Mcat strain targets, which caused a re-evaluation of its role as putative target for vaccines [93].

Among Mcat antigens, many of them are involved in nutrient acquisition: the Oligopeptide permease protein A (OppA) is engaged in peptides uptake and it is pivotal for Mcat persistence in human lungs[94]; Iron acquisition occurs through Transferrin-binding protein (Tbps)[95] and Lactoferrin-binding proteins (Lbps)[96] with a pretty similar mechanism. These bacterial receptors are localized on the outer membrane, and are able to bind human transferrin and lactoferrin facilitating iron acquisition. These proteins are composed by two subunits: integral membrane protein TbpA/LbpA forming the iron channel; and TbpB/LbpB peripheral proteins attached to the membrane by lipid draft; all subunits are involved in Human transferrin/lactoferrin binding, while only subunits A are responsible of iron transfer inside the bacteria. Iron acquisition also mediated by Catarrhalis Outer Membrane protein B (CopB)[97,98], while binding and transport of long-chain fatty acids occurs via Outer membrane protein E (OmpE)[99].

The most recent technology of genome mining has allowed identification of new Moraxella surface proteins (Msps) such as Msp22, Msp75 and Msp78[100], but also the discovery of other proteins with a not yet well-defined function (OmpG1[101]; M35[102]). Among the non-protein outer membrane components, lipooligosaccharide (LOS) represent the major virulence factor in Mcat outer membrane. LOS plays a fundamental role in inducing inflammatory responses[103,104] and is involved in the adhesion to epithelial cells[105] and in serum resistance[106].

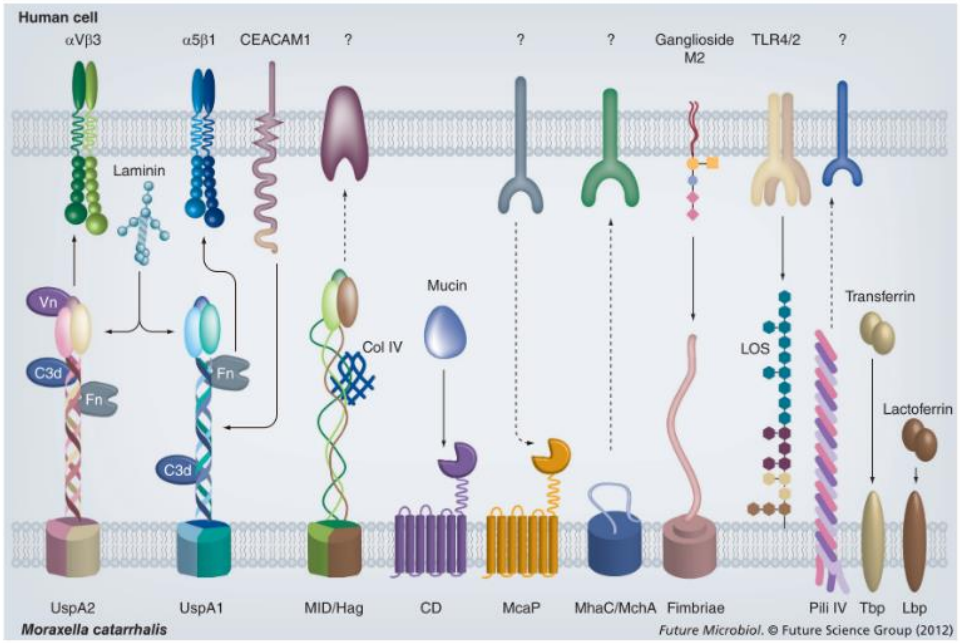


***Figure 3.*** *Adhesins of Moraxella catarrhalis interact in multiple ways with human proteins and cell receptors (Yu-Ching et al. 2012).*

### 1.4.1.2 Persistence mechanisms of Mcat

Although it has long been considered a commensal pathogen of the respiratory tract, large cohort studies have shown that *Moraxella catarrhalis* is associated with approximately 10% to 15% of exacerbations during acute COPD infection [79]. Moreover, the last 30 years have witnessed a wide spread of Beta lactam resistance among Moraxella strains, resistance that seems to have a protective effect on co-colonizing pathogens[107,108]. Anyway, Mcat-associated diseases represent a burden for health systems worldwide, prompting research towards the understanding of the mechanisms of infection to identify possible vaccine candidates.

The large variety of adhesins expressed on the bacterial surface is responsible for its significant adhesive capabilities. Phospholipids, lipooligosaccharides (LOS), integral outer membrane proteins (OMPs), and lipoproteins ensure adhesion to the respiratory epithelium through multiple interactions with different components at the host surface[77]. In addition, many of these components demonstrate a binding affinity towards extracellular matrix components[109], suggesting their involvement

into colonization of severely damaged and remodeled epithelia like in COPD subjects[110].

Following the adhesion phase, Moraxella can invade the host organism as a valid mechanism of elusion from the immune system. Several studies have demonstrated the involvement of LOS and UspAs in promoting cell invasion[111]. Likewise, interaction with specific host surface components such as fibronectin, integrins and CEACAM would also have a facilitating function during the invasion[86]. Studies conducted in vitro by Slevogt on A549 and BEAS-2B bronchial cells demonstrated an active involvement of the host into the pathogen internalization process. Electron microscopy images showed the formation of lamellipodia and filopodia due to the activation of RhoGTPase-mediated signaling on the microfilaments[87]. To date, the mechanism has not yet been elucidated.

Recently, evaluations of human specimens of adenoids, tonsils and middle ears have revealed the presence of intraepithelial structures as a possible reservoir of infection[112]. In addition, *in vitro* assays[113] and *in vivo*[114] evaluations have shown the ability of Moraxella to produce dense bacterial communities called biofilm as persistence strategy. Bacteria result embedded in a self-produced extracellular polymeric substance (EPS), which enhance nutrient capitalization, metabolite exchange and cellular communication. These robust structures confer resistance to environmental stress, antibiotics treatment and to host immune response[115]. Some exploratory studies have observed a positive correlation between the presence of the UspAs proteins[116], PilA[85], entry nuclease nucM[117] and biofilm formation, but the mechanisms underlying its formation are still unknown.

Moreover, Mcat can interfere with the host inflammatory response. The interaction of bacterial UspA1 with the host membrane protein CEACAM can interfere with TLR2-activated signaling, and the downstream activation of transcription factor NFKb and expression of pro-inflammatory cytokines[118].

Finally, it has been reported the Mcat ability to express antioxidant genes to survive to oxidative environments such as hydrogen peroxide[119] or to phagocytic vacuolar structures[120]. Moreover, the expression of nitrite reductase (AniA protein) by Mcat can act on the level of intracellular messenger oxide nitric (NO) to pathophysiological levels leading to unfunctional host cell signalling and modulation of host gene expression[121].

To date, there is no clear view of the multifactorial dynamics occurring between host and pathogen. In addition, the selective tropism of Mcat for the human mucosa makes animal models not representative and the use of simplified *in vitro* models irrelevant. Currently, no relevant animal models or *in vitro* systems capable of mimicking Mcat interaction with host tissues have been identified.

## Aim of thesis

*Moraxella catarrhalis* is recognized as one of the etiological factors involved in COPD acute exacerbation. The persistence of bacterial infections in the airways has significant implications for the progression and COPD pathogenesis. *Moraxella catarrhalis* likely causes approximately 10% of exacerbations in COPD subjects. Indeed, COPD patients continuously acquire strains of Mcat which can survive within the airways for months or years. Although Mcat is a common colonizer of the human respiratory tract, the mechanisms underlying its ability to persist within the airway system are still unclear. Moreover, the lack of suitable animal models to understand the etiology of infection make its eradication complicated and development of innovative *in vitro* alternatives urgent.

In this work, we aimed to employ highly physiological *in vitro* models fully replicating the complex architecture of human airway epithelia in order to investigate and characterize the interaction of Mcat with the human respiratory bronchial epithelium. The experimental plan was based on the use of modern fluorescence microscopy technologies, either confocal or multiplexed, for the study of Mcat interaction with human respiratory organotypic models. Moreover, initial exploratory studies were carried out to assess the gene expression profile of Mcat during infection of respiratory models alone or in presence of NTHi.

# Materials and Method

## 3.1 Human small airways *in vitro* models

Most experiments were performed using cellular models developed in-house starting from primary human epithelial cells isolated from the upper (hAEC) or lower airways of healthy or COPD-affected subjects. Alternatively, SmallAir and MucilAir models were purchased by Epithelix. The first step of respiratory models' production involves the expansion of primary cells; they were expanded in 75 $cm^2$ flasks, using human Airway Epithelial Cell Culture medium (hAEC; Epithelix) supplemented with Primocin (Invivogen), and kept at 37°C in 5% $CO_2$ until approximately 80% confluence and trypsinized using Trypsin-EDTA (0.25%) (Gibco) for seeding between passage 4 and 6.

Two different configurations were used for this work: standard and inverted; the same protocol was followed for the realisation of both model types, with some minor modifications for the inverted model, partly suggested by innovative approaches reported in the literature[122]. 6.5 mm Transwell with 0.4 µm Pore Polyester Membrane Insert (Corning product #3470) were coated with a Collagen Type I solution from rat tail (REFC3867-1V, Sigma-Aldrich) prior to seeding. Human airway cells were applied on the upside or underside of transwell; 0.5 x $10^5$ cells and ~1 x $10^5$ cells were seeded on the apical chamber of the inserts and on the underside of flipped transwell in standard and inverted configuration, respectively. After one hour incubation at 37 °C, exceeding media and untouched cells were aspirated and membrane inserts were returned in plate; 600µl and 200µl of media were added in basal and apical chambers and cultivated in submerged conditions for 3-5 days. Once a monolayer of cells was formed, cell differentiation was induced for two weeks culturing models at the Air-Liquid-Interface (ALI) with complete Pneumacult-ALI medium (StemCell Technology), with media exchange every 2-3 days. To recreate the ALI conditions, apical media were removed for standard-configured models, while in inverted models the basal chamber was drained. During this phase, the exceeding of mucus was removed with DPBS, calcium, magnesium (ThermoFisher) apical rinses. After this phase of differentiation, differentiation media was replaced with SmallAir medium

(Epithelix). In order to ensure better, complete and durable tissue differentiation, a Matrigel-embedded fibroblasts feeder layer were added on the underside (standard configuration) or upside (inverted configuration) of the porous membrane. For this purpose, Normal Human Lung Fibroblasts (ATCC) or IMR90 cell line (ATCC) were used.

Normal Human Lung Fibroblasts (ATCC) were cultured using Fibroblast Basal Medium (ATCC, PSC-201-030) supplemented with Fibroblast Growth Kit-Low serum (ATCC, PCS-201-041) and Primocin (InvivoGen) in 75 $cm^2$ flasks and used between passage 4 and 6. Before seeding, the cells were detached from the flask by trypsinisation and resuspended in 25%Matrigel in SmallAir and kept in ice. For fibroblast seeding on standard-configured models, 20µl of solution containing ~3 x $10^3$ cells were added on the underside of flipped transwell; in models with inverted configuration, 40 µl of cells solution (containing ~2.5 x $10^3$ cells) were added directly in the apical chamber. Both types of cultures were incubated at 37°C for 30 minutes to allow the solidification of Matrigel; then, transwell were placed back in plates and culture media added restoring the ALI conditions.

Human lung derived fibroblast IMR-90 were cultured in 10% FBS and primocin supplied EMEM and used for seeding between 3 and 6 passages. To use these cells as a feeder layer in co-culture systems with primary cells, an additional cell preparation step before seeding was required. Cells were γ-irradiated Gammacell 3000 irradiator (ELAN) (6000 rads) for a treatment time calculated to $^{137}Cs$ decay rate. Has been widely report that γ-irradiation can suspend DNA replication of the feeder cells by introducing double-stranded breaks in the DNA[123]. After treatment, cells were resuspended in 25%Matrigel-SmallAir solution and seeded following the same protocol illustrated for NHLF.

Full differentiation of the tissue was reached at least two weeks after the addition of fibroblasts, as confirmed by confocal scanning laser microscopy (Zeiss LSM 710) evaluation of cilia, tight junctions, goblet cells, basal cells and club cells specific markers presence. The TJ formation and cell polarity was assessed

measuring transepithelial electrical resistance (TEER) (EVOM2; World Precision Instruments).

### 3.2 Bacterial cultures and model infections

Bacterial strains used for this work: *Haemophilus influenzae* NTHi strain 1180 and *Moraxella catarrhalis* strain 415 were isolated during the prospective, observational cohort AERIS study Wilkinson et al (NCT01360398). Frozen glycerol stocks of bacteria were streaked on PoliVitex chocolate agar (bioMérieux) plates and incubated overnight at 37°C with 5% of $CO_2$. Afterward, bacterial colonies formed on agar plate were collected and inoculated in Brain-heart infusion (BHI) growth medium at 37°C, 180 rpm with 5% $CO_2$. For NTHi growth, media required supplementation of 5 μg/ml haemin and 2 μg/ml of nicotinamide adenine dinucleotide (NAD, Sigma). Bacteria were grown until mid-log phase was reached and concentration monitored by measuring O.D. at 600 nm. At 0.5 $OD_{600}$, bacteria were pelleted and resuspended in SmallAir; 100 µL and 50 µL of bacteria suspension were used to infect apical side of tissue grown in standard and inverted configuration, respectively. The number of bacteria added to each sample was ~$3 \times 10^8$ CFU/mL for Mcat AERIS 415 and ~$1 \times 10^9$ CFU/ml for NTHi 1180. Infected samples were incubated for 1h at 37°C to allow bacterial adhesion; then washed three times with DPBS to remove the unattached bacteria and placed back in plate with SmallAir without antibiotics.

### 3.3 Laser Scanning Confocal Microscopy

For confocal microscopy analysis, models were washed with DPBS and fixed with 4% formaldehyde. Then, membranes were cut with a scalpel and placed in a 48-well plate for staining. Samples were firstly permeabilized with 1% saponin (Sigma), 0.1% Triton X-100 in PBS solution for 30 minutes, then blocked with 3% bovine serum albumin (Sigma), 0.1% Triton X-100 in PBS for 45 minutes. Subsequently, membranes were incubated with primary antibodies for 1h, washed with Blocking solution, then treated with Alexa Fluor-conjugated secondary antibody or chemical probe samples for 45 minutes. Finally, membranes were mounted on microscopy glass slides and embedded with ProLong gold antifade

reagent (Thermo Fisher). Zeiss LSM 710 confocal microscope or Opera Phenix HCS Plus (PerkinElmer) were used for samples acquisition and Harmony HCI software (PerkinElmer) for Image analysis.

| **Primary antibodies** | **Manufacturer** | **Product code** |
|---|---|---|
| Rabbit anti-UspA2 | This study | N/A |
| Mouse anti-Lamp-1 | Santa Cruz technology | Sc18821 |
| Mouse anti-β-Tubulin IV | Sigma-Aldrich | T7941 |
| Rabbit anti-Uteroglobin | Thermo Fisher | PA5102469 |
| Mouse anti-MUC5AC | Sigma-Aldrich | MAB2011 |
| Mouse anti-ZO1 | Thermo Fisher | 339100 |
| **Secondary antibodies** | | |
| Mouse anti-p63 | Abcam | Ab735 |
| anti-mouse 488 | Thermo Fisher | A11029 |
| anti-rabbit 568 | Thermo Fisher | A11011 |
| anti-rabbit 488 | Thermo Fisher | A11008 |
| **Dyes** | | |
| DAPI | Thermo Fisher | D1306 |
| Phalloidin 647 | Cell Signaling | 8940S |

***Tab. 1*** *List of antibodies and markers used in this study*

### 3.4 Cell Dive imaging

For Multiplexed immunofluorescence microscopy, models were washed with DPBS and fixed with 4% formaldehyde for 24h. Then membranes were removed from transwell insert with a scalpel and placed in PBS in 1,5mL tubes and finally shipped to Stevenage at 4°C. Inserts were bisected; Half of each insert was processed and embedded by the standard FFPE method while other half was embedded in Optimal cutting temperature compound and snap frozen in liquid nitrogen cooled isopentane. FFPE blocks were sectioned at 4um and stained for H&E using the Roche HE600 automatic staining instrument (Roche diagnostic, USA). FFPE samples were baked at 65 °C for 1 h, deparaffinized with Histochoice clearing agent (Amresco), and rehydrated by decreasing ethanol concentration washes. Slides were processed for antigen retrieval with BOND Epitope Retrieval Solution 2 (Leica Biosystem) on Leica bond (Leica biosystem) for 30 min. Before antibody incubation, each slide was stained with DAPI (Sigma Aldrich) for 10 min then scanned for autofluorescence on Leica Cell Dive. Primary antibodies were incubated for 1h at RT, followed by 30 min incubation of a secondary antibodies. Third incubation was done for any conjugated primary antibodies. Imaging was performed on the Leica Cell Dive, with standard exposure times per channel (software settings: FITC 120 ms, Cy3 100ms, Cy5 150ms, Cy7 400ms). For assay 1, dye inactivation protocol was applied between round 1 and 2, followed by a second round of staining. This method provides use of Sodium hydrogen carbonate and H2O2 to inactivate Cy dyes and Alexa Fluors. The buffer was used at RT for 15 mins and repeated 3 times. Following dye inactivation, another Autofluorescence image was captured, which is used as the baseline for the second staining round. Finally, images were visualised White-in level set so that signal is detectable in HALO. Black-in set so that any residual background staining was not visible.

| Manufacturer | Host species | Product name | Labeling/conjugation | Catalogue number |
|---|---|---|---|---|
| Thermo Fisher Scientific | Mouse | PanCK_AE1/AE3 | Alexa Fluor 488 | 53-9003-82 |
| Miltenyi Biotec | Human | CD324 (E-cadherin) | PE | 130-127-980 |
| Miltenyi Biotec | Human | CD138 | apc | 130-115-480 |
| Miltenyi Biotec | Human | KRT5 | APC, REALEASABLE | 130-127-016 |
| abcam | Rabbit | KRT17 | AF488 | ab185032 |
| abcam | Rabbit | ZO-1 | unconjugated | ab221547 |
| abcam | Rabbit | beta 1 integrin | AF647 | ab225270 |
| BioLegend | Mouse | CD105 (Endoglin) | PE | 800504 |
| abcam | Rabbit | alpha 2 integrin | AF555 | ab280853 |
| abcam | Rabbit | alpha 5 integrin | APC | ab221283 |
| Thermo Fisher Scientific | Mouse | Occludin | AF488 | 331588 |
| Thermo Fisher Scientific | Mouse | Claudin 7 | unconjugated | 37-4800 |
| Thermo Fisher Scientific | Rabbit | Claudin 3 | unconjugated | 34-1700 |

***Tab. 2*** *List of antibodies used for CellDive imaging*

| Sample | Staining Assay/ Round | Dye inactivation before round | Reagent Channel 1/dilution | Reagent Channel 2 | Reagent Channel 3 | Reagent Channel 4 | Reagent Channel 5 |
|---|---|---|---|---|---|---|---|
| Ctrl Sample 1/2/3 | Assay 1 Round 1 | None | DAPI | Occludin AF488 | ZO-1 Cy3 | CLDN 7 AF647 | None |
| Mcat 48h Sample 1/2/3 | Assay 1 Round 1 | None | DAPI | Occludin AF488 | ZO-1 Cy3 | CLDN 7 AF647 | None |
| Ctrl Sample 1/2/3 | Assay 1 Round 2 | CellDive Dye inact. X3 | DAPI | panCK AF488 | CD105 PE | CD138 APC | None |
| Mcat 48h Sample 1/2/3 | Assay 1 Round 2 | CellDive Dye inact. X3 | DAPI | panCK AF488 | CD105 PE | CD138 APC | None |
| Ctrl Sample 1/2/3 | Assay 2 Round 1 | None | DAPI | KRT17 AF488 | A2 integrin AF565 | KRT5 APC | CLDN3 AF750 |
| Mcat 48h Sample 1/2/3 | Assay 2 Round 1 | None | DAPI | KRT17 AF488 | A2 integrin AF565 | KRT5 APC | CLDN3 AF750 |

***Tab.3*** *Design used for CellDive assay*

### 3.5 Bacteria complementation

A cloning strategy was designed for the generation of Moraxella catarrhalis AERIS 415 fluorescent strain. The entire strategy was thought to create a cloning vector containing the mCherry reporter gene sequence and kanamycin resistance cassette and to insert into the original bacterial genome strain relying on enzyme-free Polymerase Incomplete Primer Extension (PIPE) method [124]. *Ggt* pseudogene complementation locus was selected by analysis of Mcat BBH18 genome (KEGG database) and reported in study [125]. The strategy was composed by 4 steps: 1) cloning the whole complementation locus (comprising of 500 bp left and right flanking) in a pET15 plasmid; 2) cloning antibiotic resistance cassette (kanamycin) within the complementation locus flanking regions; 3) cloning mCherry expression cassette downwards kanamycin cassette; 4) perform site-direct mutagenesis of wild type strain with the final construct. The Kanamycin sequence was isolated from in-house bacterial genome; The mCherry cassette was composed by codon-optimized mCherry sequence and OmpCD promoter sequence (identified by Bprom promoter recognition program); the designed sequence was supplied by Twist. The procedure outline is reported in picture X.

At each step, vector and insert were linearized in PCR amplification step (GeneAmp PCR system 9700 Thermocycler) using Kapa HIFI HotStart ReadyMix DNA polymerase (KAPA biosystems) and primers (Metabion) designed following PIPE rules (including extensions of at least 15 bases complementary to the paired oligonucleotide for hybridization) reported in tab. 4. PCR products were used to transform One shot Mach 1-T1 Chemically Competent E. coli cells (Thermo Fisher) following manufacturing instructions. Colonies grown on 100ug/mL ampicillin/LB agar plates were screened using Dream Taq Green PCR Master mix (Thermo-Fisher). PCR settings were adapted to each reaction and are summarized in table 5. PCR products were analyzed on 1% agarose (Sigma) and SyberSafe (Thermo Fisher) gel electrophoresis. Plasmids positive to insert internalization were purified by E.Z.N.A. Plasmid DNA Mini Kit II (omega) and final construct sequenced at GSK Sequencing facility according to Sanger method using a 96-capillary ABI 3730xl DNA Analyzer. The final cassette obtained in step n.3 was amplified using

Kapa HIFI HotStart ReadyMix DNA polymerase (KAPA biosystems) and purified with a Wizard SV Gel and PCR clean up system (Promega). The purified construct was incubated with wild type Mcat for 6 hours at 37 °C to allow homologous recombination before being tested on kanamycin treated agar chocolate plates. Colonies expressing resistance to kanamycin and pink color were selected and screened to verify construct insertion. Primers annealing upstream and downstream the complementation locus *ggt* on wildtype Mcat genome and transformed colonies were used to amplify by PCR the selected region. Products were analyzed by gel electrophoresis (Fig. 5a); all colonies tested confirmed the correct integration of construct within the selected region of genome. Frozen stocks of transformed strains (16% glycerol) were created and stored at -80 °C.

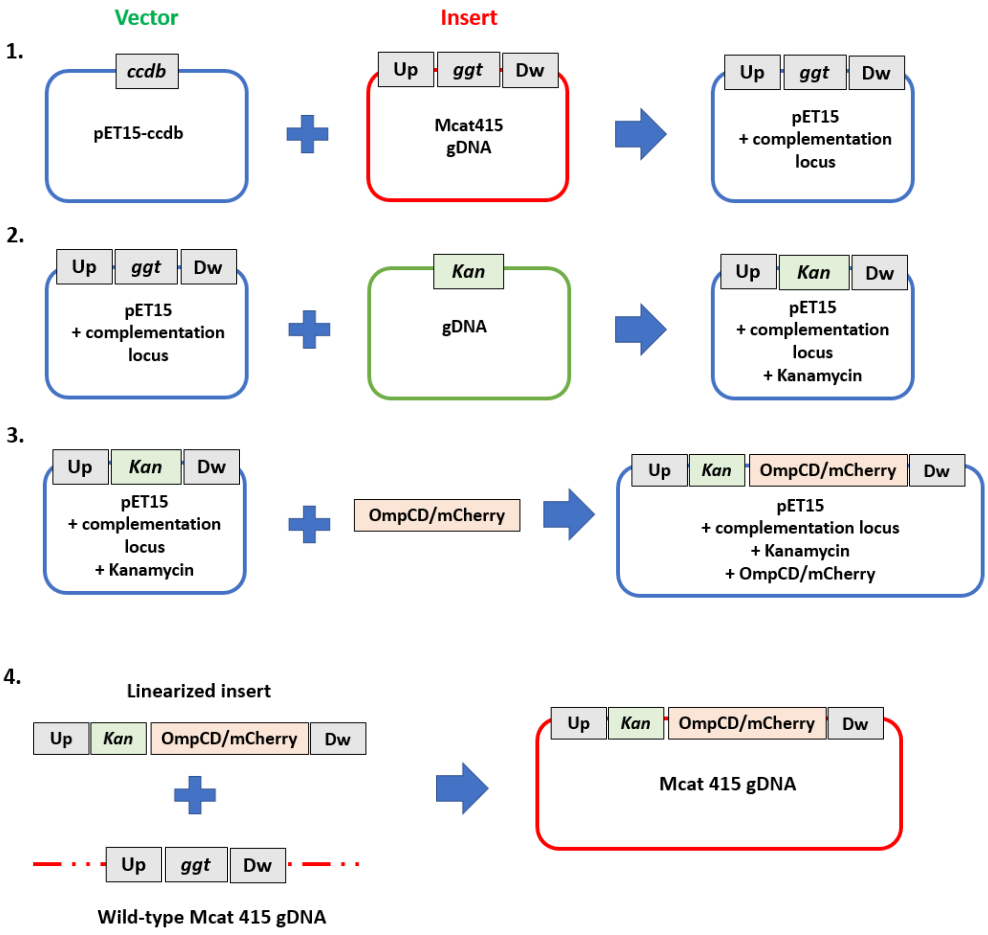


***Figure 4*** *Cloning strategy design for mCherry complementation in the Moraxella catarrhalis genome 4*

| Primer | Sequence (5' - 3') | Step |
|---|---|---|
| **V-PIPEUniv F** | TAACGCGACTTAATTGGCCAGTGTGCCGGTCTCCG | 1.V-PIPE |
| **pET15Korv** | GACTCACTATAGGGGAATTGTGA | 1.V-PIPE |
| **ggtUPfw** | ATAGGGGAATTGTGACGATACGGTGTATTGCCTTGG | 1.I-PIPE |
| **ggtDOrv** | CCAAGATGCCATCAGTGCACTAACGCGACTTAATT | 1.I-PIPE |
| **ggtDOfw** | CTGTACCCATTCGCCAGTTG | 2.V-PIPE |
| **ggtUPrv** | CCTTCAGCATCATACCCCACC | 2.V-PIPE |
| **Kana-UpFw** | GTATGATGCTGAAGGATGCCGTCTGAAGGATCC | 2.I-PIPE |
| **KanaDwRev** | GGCGAATGGGTACAGTATCCATGGGGATCCTCATTATTC | 2.I-PIPE |
| **ggtDOfw** | CTGTACCCATTCGCCAGTTG | 3.V-PIPE |
| **KanKOR3** | TATCCATGGGGATCCTCATTATTC | 3.V-PIPE |
| **OmpCDkanafw** | GGATCCCCATGGATATGCGTTAGAAAGAAAATCGTAAATAATG | 3.I-PIPE |
| **mCh2 Rev** | GGCGAATGGGTACAGGATCCTCTAGATTATTTATAAAGTTCATC | 3.I-PIPE |
| **McUPfw** | CGATACGGTGTATTGCCTTGG | 4.Insert linearization |
| **McDOrv** | GTGCACTGATGGCATCTTGG | 4.Insert linearization |
| **ggt LO F** | GTGGGTACGCCTGCTATCC | Colony screening (Mcat) |
| **ggt RO R** | CCATTGGACGGCGGTTGTATCC | Colony screening (Mcat) |
| **T7 PROM** | TAATACGACTCACTATAGGG | Colony screening (E.Coli) |
| **SeqPetRev** | GATATCCGGATATAGTTCCTC | Colony screening (E.Coli) |

***Tab.4*** *List of primers used for bacterial complementation strategy*

| | Temp (°C) | Time | |
|---|---|---|---|
| Initial denaturation | 95 | 5' | |
| Denaturation | 95 - 98 | 30'' | 25-30X |
| Annealing | 55 - 70 | 30'' | |
| Elongation | 72 | 30'' - 3'30'' | |
| Final elongation | 72 | 0 - 5' | |

***Tab.5*** *PCR setting for mCherry complementation strategy*

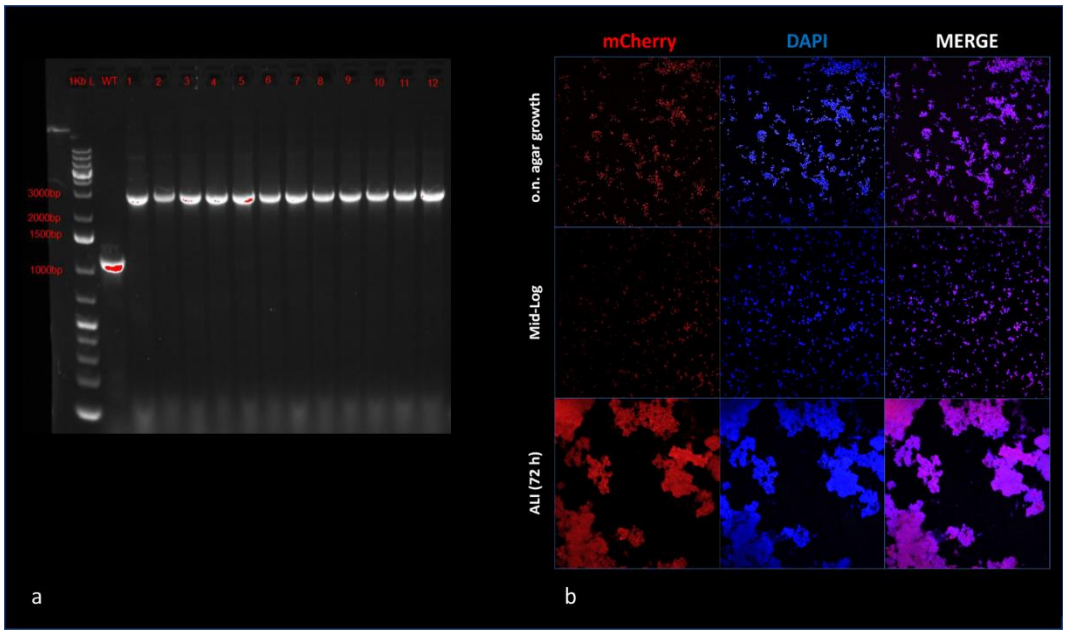


***Figure 5**. a) Agarose gel electrophoresis of colony screening PCR products: successful integration of the final construct was observed for all the screened colonies. b) Transformed Mcat strain fluorescence tests. The higher signal intensity was observed in bacteria grown at the air-liquid-interface*

Subsequently, transformed clone were analyzed by confocal microscopy to evaluate bacterial fluorescence in different growing conditions: overnight on chocolate agar plate; in BHI liquid broth reaching the mid-log phase (0.5 $OD_{600}$); and the Air-Liquid-Interface in the apical chamber of transwell inserts. Fluorescent signal looked evenly express within the entire population for solid and liquid growth; however, the fluorescence intensity was much higher for mid-log growth bacteria. Higher fluorescence was observed in bacteria grown at the Air- Liquid-Interface in the apical chamber of transwell inserts, suggesting that the intensity is related with the quantity of bacteria (Fig.5b). However, for bacteria infecting trachea-bronchial epithelial tissue *in vitro* fluorescent signal was not uniformly express and intensity too low at different stages of infection (Fig.16). In conclusion, the OmpCD promoter allowed the expression of the mCherry reporter gene under abiotic growth conditions, whereas during active infection of the epithelium its expression was heterogeneous and low.

### 3.6 RT-qPCR

After 1h of infection, bronchial models infected with Mcat 415 and Mcat415/ NTHi1180 co-infected and corresponding mock controls (three replicates per time point) were lysed in 300µl of TRI reagent (Zymo research). At same time, planktonic bacteria were conditioned in infection media for 1h at 37°C in 5% $CO_2$ then were lysed and used as bacterial control. Direct-zol RNA Microprep Kit (Zymo research) was used to extract total RNA according to manufacturer's protocol. After a first step of purification and DNase treatment on column, a further step of DNA removal in liquid was performed using TURBO DNA-free kit (Thermo Fisher). To remove any reagent excess, a second step of RNA purification on column was done. Purified RNA samples were firstly quantified using a Nanodrop ND-1000 (Thermo Fisher) then quality was evaluated using Agilent 2100 Bioanalyzer. Microchip Gel Electrophoresis was done by Agilent RNA 6000 Nano kit, following manufacturer instructions. Once assessed the high quality of extracted RNA, 1 µg of total RNA for each sample was reverse transcribed to complementary DNA (cDNA) using the Superscript IV Reverse Transcriptase Kit (Thermo Fisher). Each 25µl real time PCR mixture consisted of 0,5µl of each primer (Metabion; reported in tab. 6), 12,5µl of Platinum SYBR Green qPCR SuperMix-UDG with ROX (Thermo Fisher), 10,5 µl of DEPC-treated water, 1 µl of total RNA (2,5 ng/ µl). qPCR was carried out on Stratagene Mx3005P system applying setting reported in tab 7. The relative expressions of the selected genes were studied and estimated based on the relative $2^{-\Delta\Delta CT}$ method using conditioned bacteria as reference [126].

| Protein | Gene symbol | KEGG Reference Genome/ Locus tag | Sequence | Amplicon size (bp) |
|---|---|---|---|---|
| Ubiquitous surface protein | UspAH | T01224 MCR_0329 | Fw_GCGTCTGCACAAGTAGTAGGC<br>Rv_CGATATTAAAAAAGCCACCACC | 117 |
| Pilin protein subunits | FimA | T01224 MCR_0392 | Fw_CCATACCTCAATACCAAAAACG<br>Rv_AGTAGACACATTTCAACAGCCG | 97 |
| sulfate-binding capacity ATP-binding cassette (ABC) transporters | CysP | T01224 MCR_0896 | Fw_AATGTTTCTTACGATGTGTCTCG<br>Rv_TTTTGGTATTTGGGTAGTTGGTC | 91 |
| Transferrin-binding proteins | TbpA | T01224 MCR_0690 | Fw_CGAAGTTACAGGGCTTGGTAAG<br>Rv_AGGGTCATAGCGTGTTAAGTCTC | 94 |
| DNA/RNA non-specific endonuclease | NucM | T01224 MCR_1533 | Fw_GCTATGGTCAGCATCTCATCTG<br>Rv_CATCAGCAGGTAGTCTGGACTC | 99 |
| Beta-lactamase family protein | blaP | T01224 MCR_0463 | Fw_GGTCAAGAGGTGGTTAATACC<br>Rv_TCAGAGACAAGCACGGC | 131 |
| 16S ribosomal RNA (Mcat) | 16S | T01224 MCR_1955 | Fw_CCATCGGTATTCCTCCAGATCTC<br>Rv_GGGAACTGCATCTGATACTGGAT | 100 |
| 16S ribosomal RNA (NTHi) | 16S | T00248 NTHIR0003 | Fw_CCTGGGAATTGCATTTCAGACT<br>Rv_CGGTATTCCTCCACATCTCTACG | 99 |

***Tab 6**. Primer sequences and amplicon size of the differentially expressed genes used in the qPCR reaction.*

| Step | Temperature | Time | Cycles |
|---|---|---|---|
| **UDG incubation** | 50°C | 2 minutes | X1 |
| **Initial denaturation** | 95°C | 2 minutes | X1 |
| **Denaturation** | 95 °C | 15 seconds | X 40 |
| **Annealing** | 60°C | 30 seconds | |
| **Melting curve** | 95°C | 1 minute | X 1 |
| | 55 °C | 1 minute | X1 |
| | 95°C | 30 seconds | X1 |

***Tab 7**. qPCR cycle setting*

### 3.7 Hematoxylin and Eosin

The tissue inserts were fixed O/N in 4% buffered formaldehyde pH 7.6 (Sigma-aldrich), then membranes were removed from the transwell insert with a scalpel and put in PBS for shipping at 4°C. Membranes were bisected along the sagittal plane. Half of each insert was processed and embedded by the standard FFPE method. Half of each insert was embedded in Optimal cutting temperature compound and snap frozen in liquid nitrogen cooled isopentane. and processed for paraffin embedding. FFPE blocks were sectioned at 4um and stained for H&E using the Roche HE600 automatic staining instrument.

### 3.8 Protein Phosphorylation array

The relative phosphorylation level of molecules involved into TGFβ signaling was determined using RayBiotech phosphorylation kit (AAH-PPP-1-2), following manufacturer procedure. It is a semi-quantitative, sandwich-based assay that can detect several different proteins using a chemiluminescent method. Protein-specific antibodies are immobilized onto a nitrocellulose membrane. Five infected and five mock-infected tissues equivalents were lysed using buffer provided by the kit. After complete homogenization, the suspension was centrifuged for 10 min at 14,000 g. Then, supernatants were transferred and quantified using Pierce™ BCA Protein Assay. Samples were diluted at same concentration and incubated of 100µg/mL overnight at 4°C on nitrocellulose membranes. After two washing, membranes were incubated with horseradish peroxidase (HRP)-labeled anti-rabbit secondary antibody at RT for 2 h. Signals were detected by Chemidoc® touch imaging system (Biorad). For data analysis, numerical densitometry data were extracted with microarray quantification and analysis software ImaGene 9.0 (Arrayit corporation). Subsequently, the background subtracted, and each array was normalized for its positive control.

# Results and Discussion

## 4.1 Organotypic air-liquid-interface (ALI) airway models produced in house closely mimic structures and functions of airway epithelium

Development of pseudostratified tissues alongside with expression of tissue specific cell types and functional junctional complexes is essential for creation of accurate and physiological *in vitro* systems. In order to produce highly physiological human respiratory equivalent tissues, human-derived primary cells isolated from healthy subjects were co-cultured with human fibroblasts on porous inert supports to reproduce the epithelium and stromal tissue of human trachea-bronchial mucosa. Specifically, primary epithelial cells were cultured at air-liquid interface for two weeks, then a fibroblast layer was seeded on the opposite site of the transwell membrane supporting proliferation, spatial distribution, mucus secretion and differentiation completion of the overlying epithelial tissue[127,128] (Fig. 6a).

After 30 days of culturing, models were characterized by confocal laser scanner microscopy (CLSM) for specific markers of the most representative cell types of human trachea-bronchial respiratory tract: basal cells (p63), ciliated cells (B-tubulin IV), goblet cells (MUC5A) and Clara cells (uteroglobin). Ciliated cells were widely represented covering almost the entire surface of the samples; Cilia rhythmic movement, that in synergy with mucus produced by goblet cells contribute to microorganisms, and debris expulsion[6], was clearly observable in differentiated tissue. Basal, goblet and Club cells resulted evenly distributed throughout the sample area in accordance with their localization in human respiratory epithelium *in vivo*. For their function of stem cells, basal cells are tightly secured to the basement membrane and spread along distal-proximal axis of airways; their proper distribution is pivotal for respiratory homeostasis and epithelial regeneration following injury[4]. Finally, Club (or Clara) cells represents a versatile component of epithelial tissue; besides their secretory function as surfactant producer, these cells are able to act as stem cell and aid in cell repairs[129] (Fig.7).

Confocal tomography of samples highlighted the pseudostratified structure and polarity of tissue evident by observation of F-actin distribution (Fig. 6c). Furthermore, the formation of an intact tissue epithelial barrier was assessed by monitoring Trans-Epithelial Electrical Resistance (TEER) (Fig.6b) and imaging of TJ component zonula occludens 1 (ZO-1) which was properly distributed at the apical side of tissue (Fig. 6d).

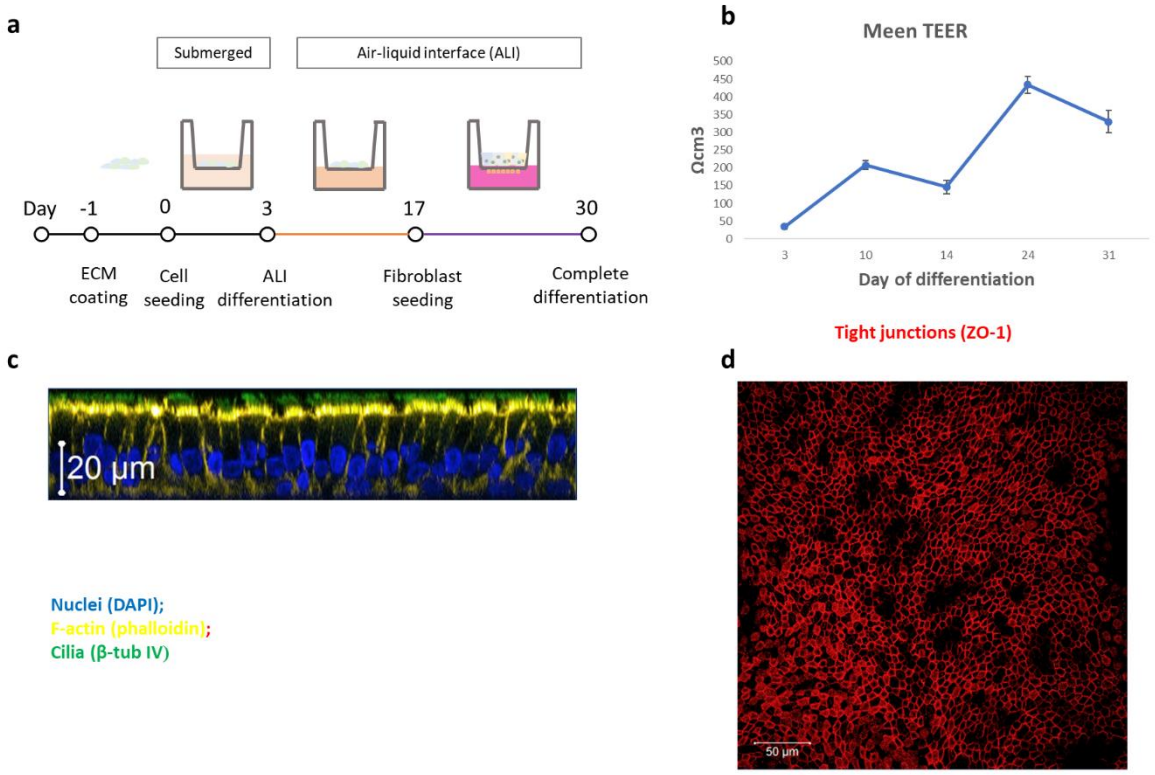


***Figure 6*** *– a) differentiation protocol used for generation of organotypic air-liquid-interface (ALI) airway models; b) Trans-Epithelial Electrical Resistance (TEER) measurements of respiratory models during the differentiation period to assess epithelial barrier formation. Results are expressed as mean values and standard deviation calculated on 8 replicates for each time point; c) Z-stack picture of models at the end of the differentiation period. Immunofluorescence staining of nuclei (blue), F-actin (yellow), cilia (green); d) Visualizing tight junctions (ZO-1, red) formed in fully differentiated tissues.*

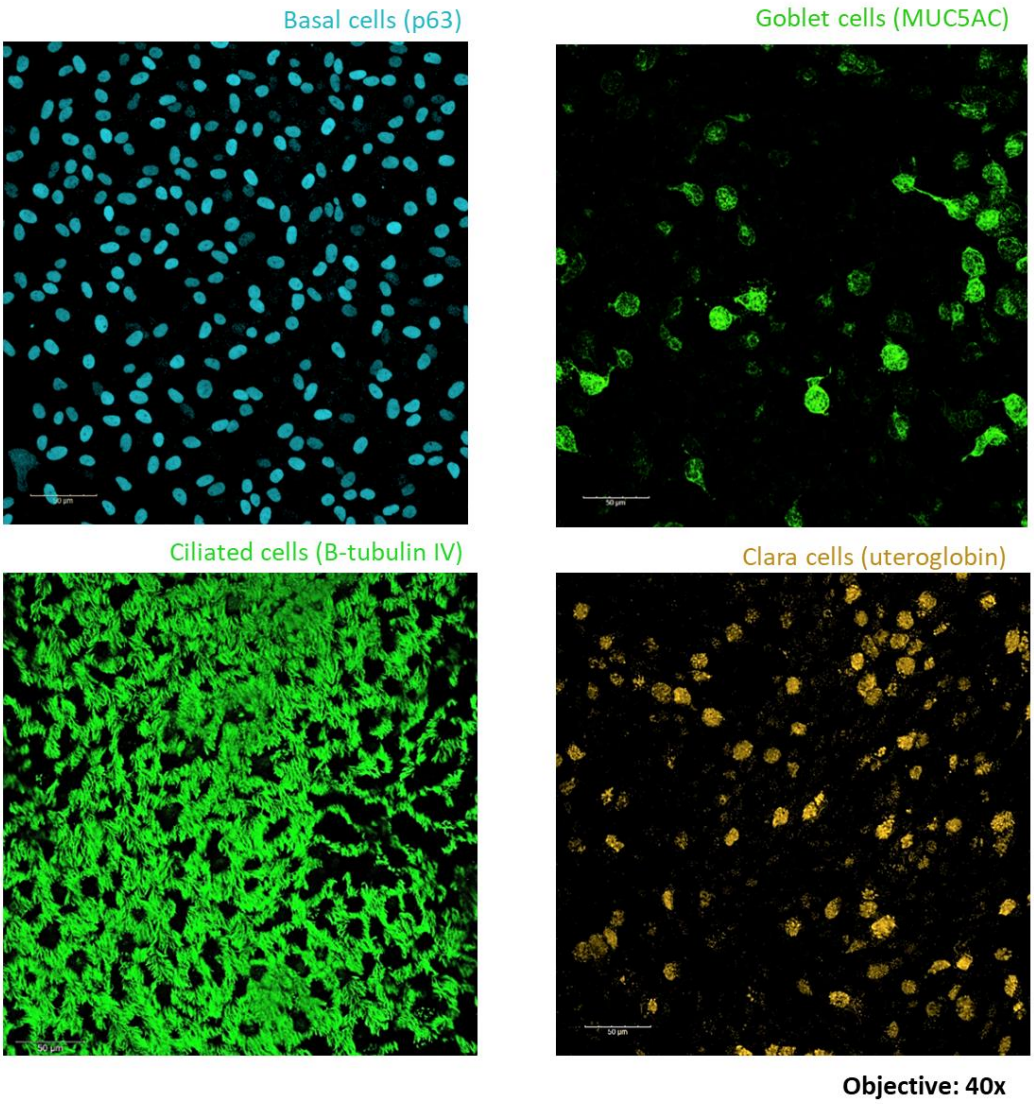


***Figure 7 -*** *confocal images of basal, goblet, ciliated and Clara cells present in an organotypic air-liquid-interface (ALI) airway models.*

## 4.2 The coinfection with NTHi influences the expression of Mcat virulence factors in the early stages of infection

Bacteria pathogens have evolved a wide variety of proteins, called adhesins, to interact with human specific surface components. These binding events dictate the species-specificity of interaction as well as the cell type tropism of microbes. *Moraxella catarrhalis* (Mcat) possess several outer membrane proteins (OMPs), that can interact with multiple cellular and matrix components[130]. However, the common use of simplified *in vitro* systems based on cancer originated cell lines (A549[130,131], Detroit[132], Chang[111]) does not allow to recreate the complex physiology of the respiratory system.

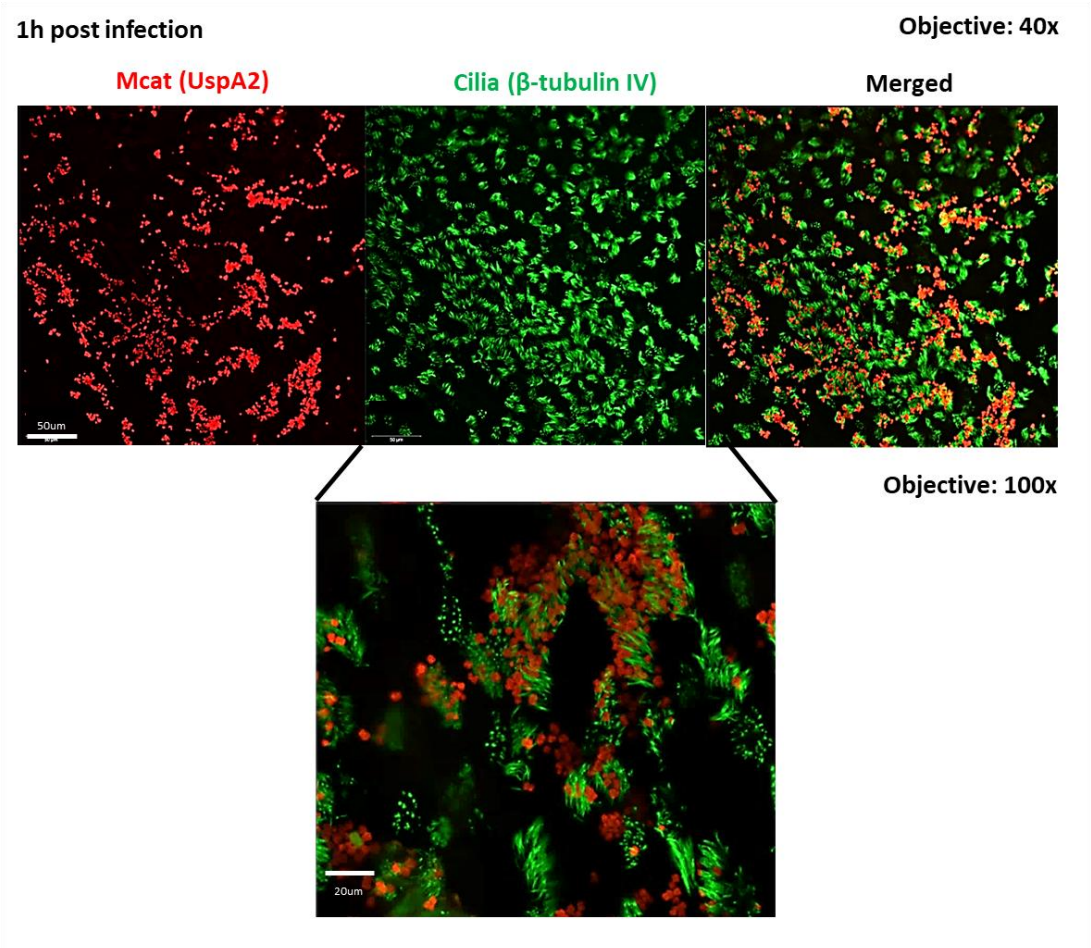


***Figure 8*** *– Mcat interaction with cilia on host epithelium after 1h of infection, 40x and 100x magnification.*

For this reason, cultures of airway epithelial cells differentiated at air-liquid interface (ALI) were employed to explore the host-pathogen interplay. Models were infected with MCat GSK415, and after 1h of adhesion, they were fixed and stained for Confocal Laser Scanner Microscopy (CLSM) observations. The analysis of bacterial adhesion on host epithelium showed ciliated cells as preferential target of adhesion; observations made at higher magnifications displayed the formation of multicellular grape-like aggregates (Fig.8) confirming previously identified tropism of Mcat for ciliated cells[130].

The host-pathogen interaction is a dynamic process where bacterial transcriptional reprogramming is central for a successful infection of the tissue. In fact, the pathogen faces adverse conditions such as lack of nutrients or different temperatures modulating the expression of various virulence factors[132]. In order to increase the understanding of bacterial strategies exploited during the first critical step of colonization recreated in complex and physiological context, we evaluated the differential expression of a selected set of genes already identified as relevant virulence factors[81–83,103] by quantitative real-time PCR (qRT-PCR). For this scope, respiratory *in vitro* models were infected with Mcat GSK415 for 1h to allow bacterial interaction and adhesion to host cells; afterwards samples were washed twice to remove not adhering bacteria and lysed in TriReagent. RNA was finally extracted, quantified and quality checked before to proceed to cDNA synthesis. Samples were then analyzed by qPCR and $C_t$ of each gene was evaluated by the Livak $\Delta\Delta C_t$ method using planktonic bacteria conditioned in infection media as control. The interaction with epithelial cells induced a significant change in expression of some genes compared to the planktonic phase control (Ctrl). Contrary to what expected, expression levels of *uspA2* (variant A2H) decreased in the first phase of interaction with the respiratory model (Fig. 9a). Although unexpected, this result can be explained by the fact that Mcat UspAs are phase-variable genes which expression can be switched during conditions such as biofilm formation and multiple exposure to human serum[81,133,134].

Similarly, a reduction in expression of the non-specific endonuclease nucM gene (*nucM*), involved in bacterial competence and aggregation[117], was observed, as well. Conversely, the expression of the outer membrane Transferrin-binding proteins subunit A (TbpA) increased during the early steps of colonization, suggesting an adaptative strategy to survive in hostile and iron-restricted environment[135]. These data suggest that Mcat, during the initial interaction with the host modulates its ability to interact with host cells and to incorporate metabolic factors essential for its survival.

Growing body of evidences report the co-existence of NTHi and Mcat during COPD[136] and otitis media pathogenesis[137]. Indeed, Mcat presence seems to promote survival of NTHi during the pathogenesis conferring NTHi resistance to complement-mediated killing *in vitro* [138], increase resistance to antibiotic treatment and host clearance of biofilms[107,139]. Therefore, we decided to analyze the expression of Mcat relevant virulence factors during initial phase of host colonization in co-infection with NTHi. Data did not indicate any synergistic effect on *UspA* gene whereas an increasing trend in expression was detected for *NucM* and *TbpA* genes in co-infected samples. Interestingly, also the expression trend of beta lactamase-expressing gene was affected by NTHi presence. These preliminary data further support the hypothesis of a possible synergistic effect existing between the two pathogens during the colonization phases of the tissue enhancing bacterial virulence and persistence strategies.

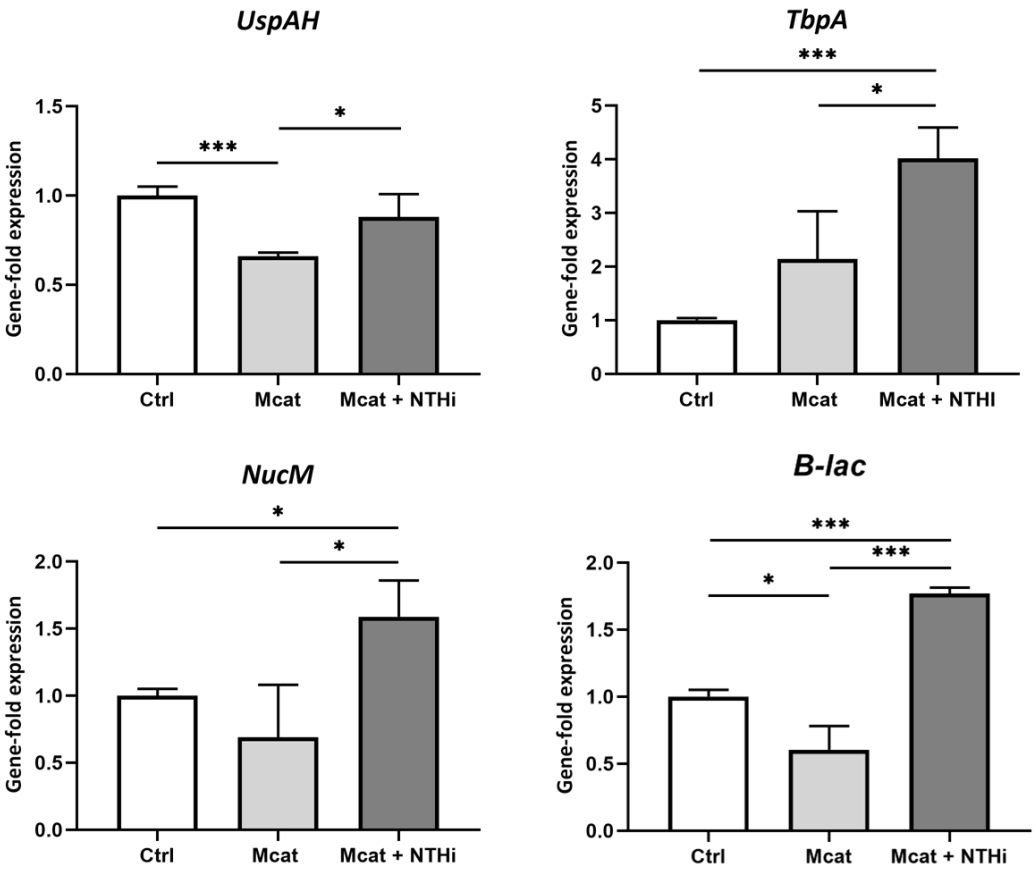


***Figure 9***. *Expression of Mcat virulence factors during first phase of infection alone and in co-infection with NTHi evaluated by qPCR. Ct of each gene was evaluated by the Livak ΔΔCt method using planktonic bacteria conditioned in infection media as control. The values are represented as the mean and standard deviation calculated of three independent samples. Significance was established using two-tailed Student's t test (*P < 0.05, **P < 0.01, ***P < 0.001). All statistical analyses were performed with Prism 8.*

### 4.3 Moraxella catarrhalis invade bronchial epithelial models with active involvement of host cytoskeleton

Bacterial anchoring to eukaryotic membrane components induces receptor binding and triggering of host signaling. The consequences of this contact are a wide variety of cellular responses from change in cell morphology, cytoskeleton remodeling to modulation of gene expression[140]. Therefore, many pathogens have evolved strategies to subvert actin filaments and induce cytoskeleton rearrangement for host invasion[141–144]. An extensive variety of adhesins covering Mcat surface can interact with epithelial cell receptors inducing bacteria internalization. Slevogt et al. identified the involvement of eukaryotic microfilaments into the macropinocytosis of bacteria as a result of a trigger-like invasion mechanism induced by the pathogen[87] in BEAS-2B and A549 cell lines.

With the use of elaborated *in vitro* assembled trachea-bronchial models and confocal microscopy technologies was possible to elucidate the early stages of Mcat colonization. After the initial phase of adhesion and adaptation to the host environment, bacteria were internalized within the tissue. Approximately after three hours, signs of host cytoskeleton recruitment at the entry site were evident. F-actin was stained with phalloidin (yellow) and Mcat labeled with an αUspA2 antibody (red). Confocal images showed a network of directionally branched F-actin underneath the pathogen, forming a phagocytic cup-like structure (Fig.10a), along with membrane ruffles formation (Fig.10b) and bacteria engulfed within (Fig.10c). Ruffles and filipodia are widely used by host to sweep and probe the environment in search of foreign objects[145]. Moreover, filamentous actin also allows endosomal trafficking regulation by recruiting several proteins, such as Rab effectors for intracellular phagosome maturation[146]. During the initial phases of Mcat infection it was possible to detect internalized bacteria surrounded by F-actin signal (Fig. 11a) indicating an active ingestion of the pathogen by epithelial respiratory cells.

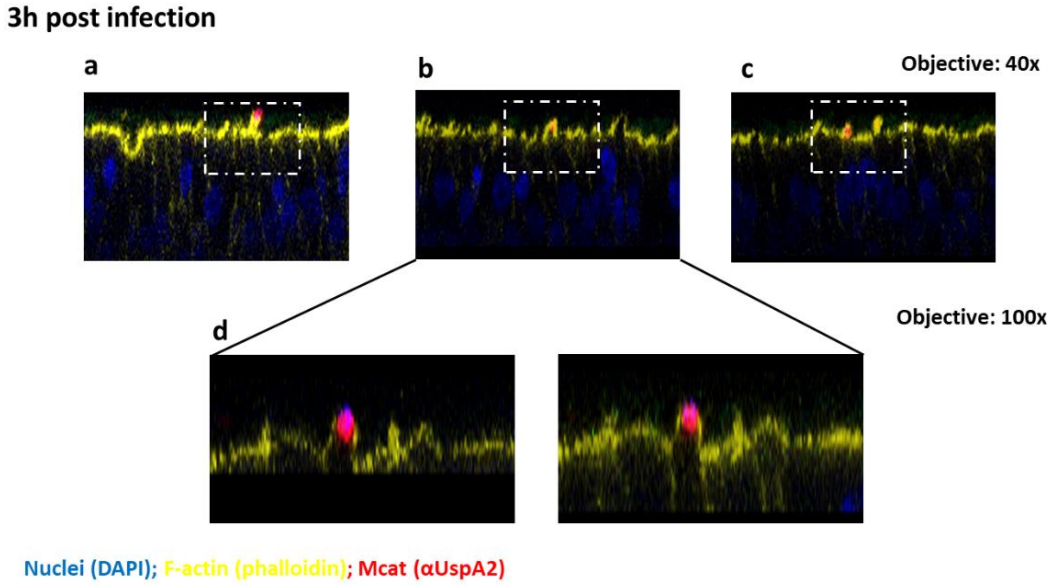


***Figure 10.*** *Z-stack pictures of Mcat (red) interaction with F-actin (yellow) after 3h of infection. A network of directionally branched F-actin formed around the pathogen, forming a phagocytic cup-like structure (a), membrane ruffles (b) and engulfed bacteria (c). Pictures in d show membrane ruffles formation around the bacteria with 100x magnification.*

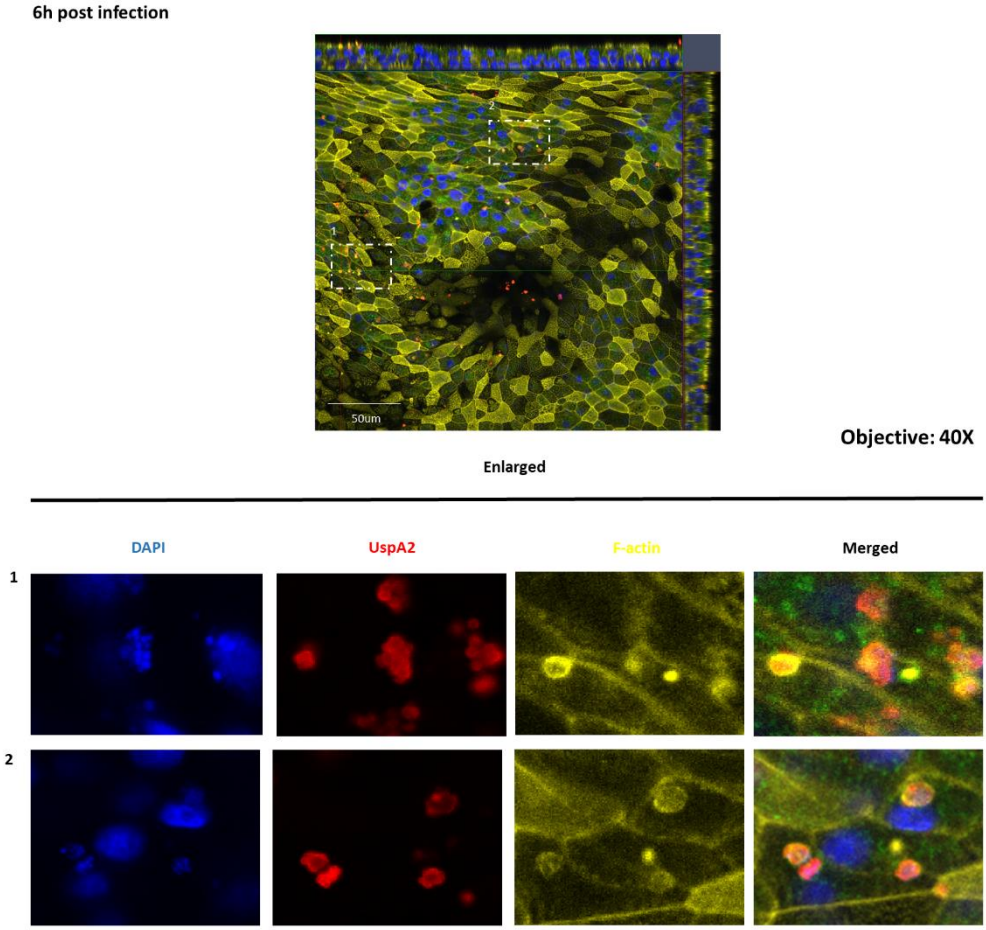


***Figure 11****. After 6h, Mcat (red) is internalized within the tissue. Enlargements of the internalized bacteria highlight small bacteria aggregated surrounded by F-actin structures (yellow).*

Previous evidences demonstrated that Mcat can reside inside vacuoles after macropinocytosis in professional[120] and non-professional cells[87,147]. In order to localize internalized bacteria within subcellular compartments confocal analysis highlighted the specific co-localization of Mcat with the late endosome marker Lamp-1 (Fig.12b), suggesting the effective delivery of ingested bacteria to canonical pathway of phagolysosome maturation. Nevertheless, small dense aggregates of intracellular bacteria were visible already after 6h of infection suggesting the hypothesis that Mcat could bypass host clearance and duplicate intracellularly (Fig.12c). According to previous studies, Mcat can express antioxidant genes to resist to oxidative environments [119] but also to replicate within vacuolar structures of immune cells or even inhibit the phagocytosis process[120]. To date, the subversion mechanism by which Mcat can escape phagocytic clearance is still elusive.

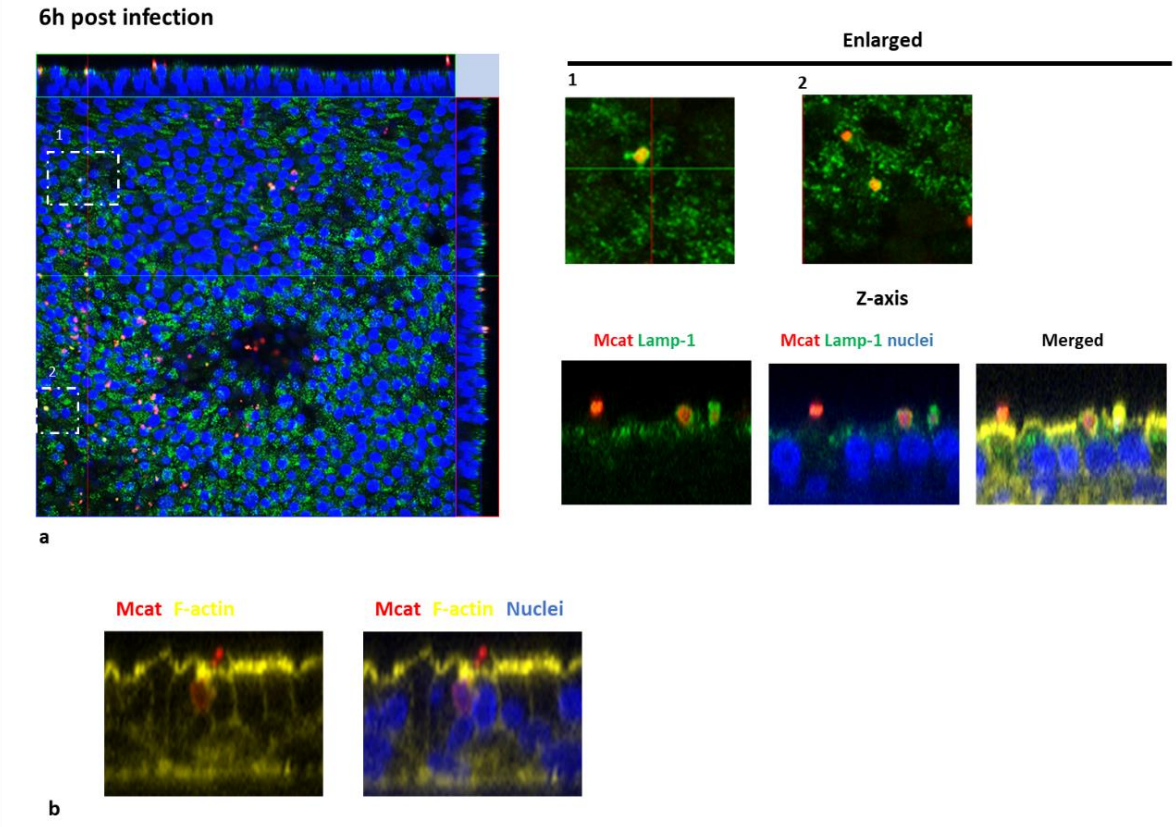


***Figure 12***. *After 6h of infection, internalized Mcat (red) co-localize with late endosome marker LAMP-1 (green) in some regions (a); enlargements and z-stack pictures of these regions highlight LAMP-1 signal surrounding bacteria in apical side of the tissue. Presence of bacterial aggregates identified by DAPI staining (blue) surrounded by anti-UspA2 signal (red) (b).*

## 4.4 Moraxella catarrhalis forms intraepithelial bacterial communities

In order to better characterize the course of infection after the initial invasion of the tissue, we evaluated samples infected for periods of time between 24 and 48 hours with confocal microscopy. Analysis of fig.13 showed that, after the appearance of small dense intracellular colonies, large bacterial aggregates expand within infected epithelial cells. Interestingly, despite the deep permeabilization of the tissue to immunostaining intracellular bacteria, these structures appeared recalcitrant to labeling that was restricted to the apical and peripheral regions only. These dense microbial structures appeared permeable only to small compounds such as DAPI which was capable to reach the core region (Fig.13, white arrows). Hematoxylin and eosin staining along with transmission electron microscopy analysis confirmed the presence of bacterial biomass expanding within the epithelia at the selected time point of infection (Fig.14 a, b). Since a similar mechanism had never been observed for Mcat in *in vitro* systems, its interpretation leaves open to various speculations and preliminary considerations.

It is reported in literature that in order to counteract to bacterial infection and preserve barrier integrity, compromised cells are extruded from the tissue by the formation of an actinic ring created by adjacent cells [54,148]. Nevertheless, Mcat-infected cells remained tightly anchored to adjacent cells and tissue matrix assuming the involvement of some pathogenic mechanism that prevents cell exfoliation from the epithelium. Intriguingly, growing biomasses appeared to cause cell swelling and breaking of apical cellular membrane (Fig. 13), concurrently with filamentous actin depolymerization. These evidences indicating the manipulation by Mcat of natural epithelial clearance processes such as intracellular bacterial digestion and exfoliation of infected cells. Furthermore, this observation suggests the engagement of articulated and yet unidentified mechanisms of cell control implemented by the pathogen distinct from apoptosis observed using A549 cell line in previous studies[149]. Until now, very few studies conducted on biopsy specimens

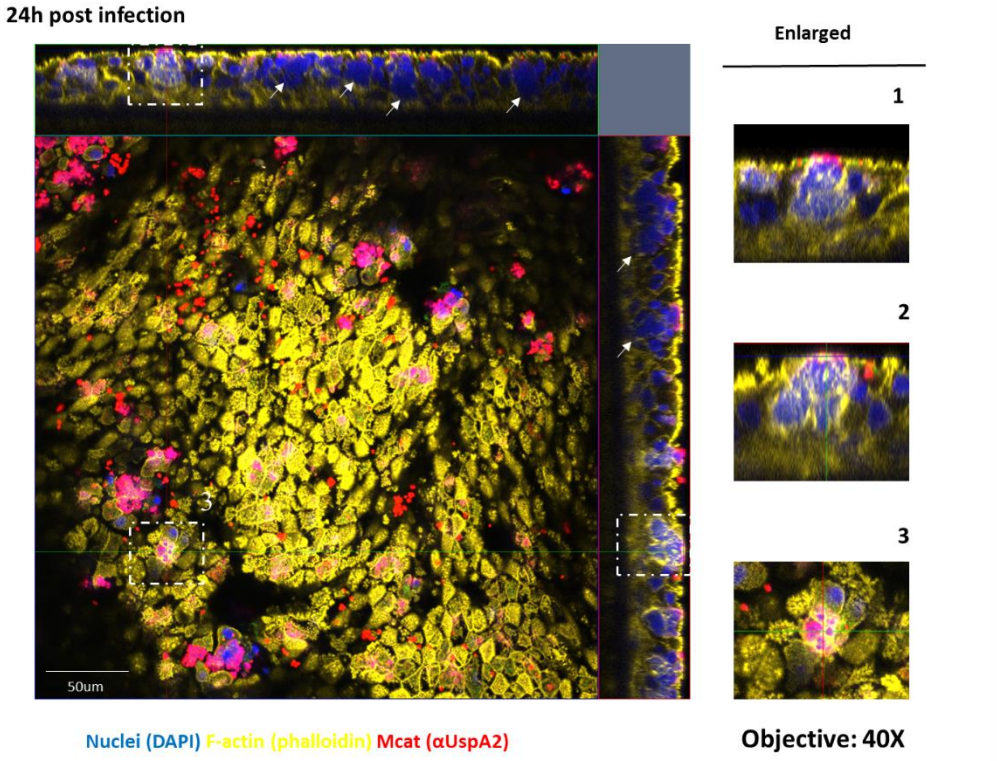


***Figure 13***. *Formation of bacterial intraepithelial communities. Pictures 1 and 2 show enlargement of Z-axis section of tissue where bacterial colony cause actin fragmentation; Picture 3 shows the bacterial colony from the top. White arrows point bacteria intra-tissutal colonies.*

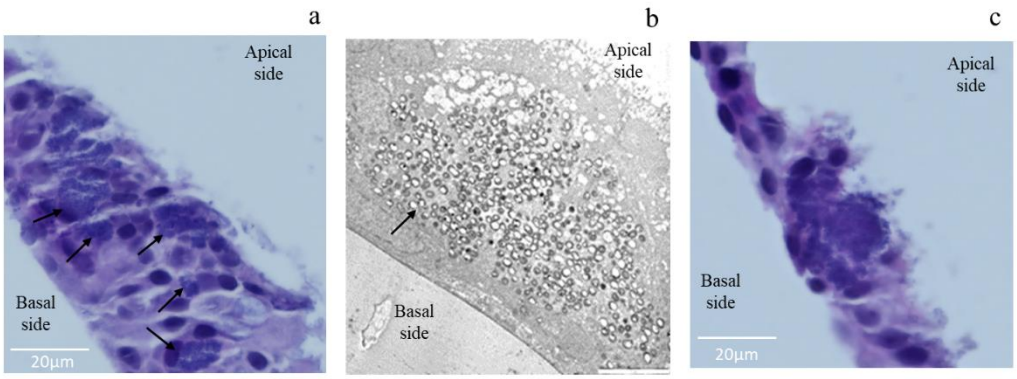


***Figure 14.*** *Picture a and c show bacterial intraepithelial communities (black arrows) and surface associated bacterial colonies stained with hematoxylin and eosin, respectively. Picture 2 shows tissue section with large number of bacteria (Black arrow) acquired at TEM.*

isolated from children with chronic middle ear infections highlighted the presence of intraepithelial biofilms, proposing this strategy as key factors behind the establishment of chronic infections[114,150].

With the progression of infection, these biofilm-like structures appeared also in association with the surface of the epithelium suggesting that intracellular bacterial colonies could serve as reservoir for the establishment of a more severe state of infection of the respiratory epithelium or the beginning of an epithelial-associated extracellular biofilm (Fig. 14c; Fig. 15). The tissue region underlying newly formed colonies appeared damaged and the epithelium strongly remodeled as highlighted by the progressive focal sections of infected samples (Fig. 15 white arrow).

Finally, in order to have the possibility to observe bacteria without the use of immunolabeling, we developed a strategy for the generation of Mcat GSK415 strain constitutively expressing the fluorescent protein mCherry. Although the insertion of the mCherry expression cassette into the bacterial genome was successful, the fluorescent intensity signal reached detectable values only when bacteria were grown in abiotic conditions (see Materials and method). On the contrary, imaging of the fluorescent Mcat mutant strain during infection was difficult since bacteria were scarcely visible with fluorescence and not all the population seemed to express the marker. (Fig.16). Nonetheless, time-lapse imaging done using Opera Phenix Plus HCS System, allowed to capture multiple images of the same region giving a temporal view of Mcat infection within the first 72 hours of infection (Fig.16). First signs of bacterial aggregate formation were evident already after 12 hours. Growing colonies emerged from the epithelium and continued to grow forming large and dense structures. After 48h the bacterium covered almost the entire surface of the analyzed sample region, which appeared highly remodeled.

Independent infection experiments conducted with multiple Mcat strains (BBH18 and Mcat AERIS GSK415) and using models produced with primary cells derived from different donors always resulted in the formation of extracellular bacteria macro-colonies within 48 hours from the beginning of the infection. The

reproducibility of this infection phenotype with different strains and donors strongly supports the hypothesis that what observed *in vitro* could potentially represent a new hallmark of a persistency mechanism adopted by Mcat during colonization of the human respiratory epithelium.

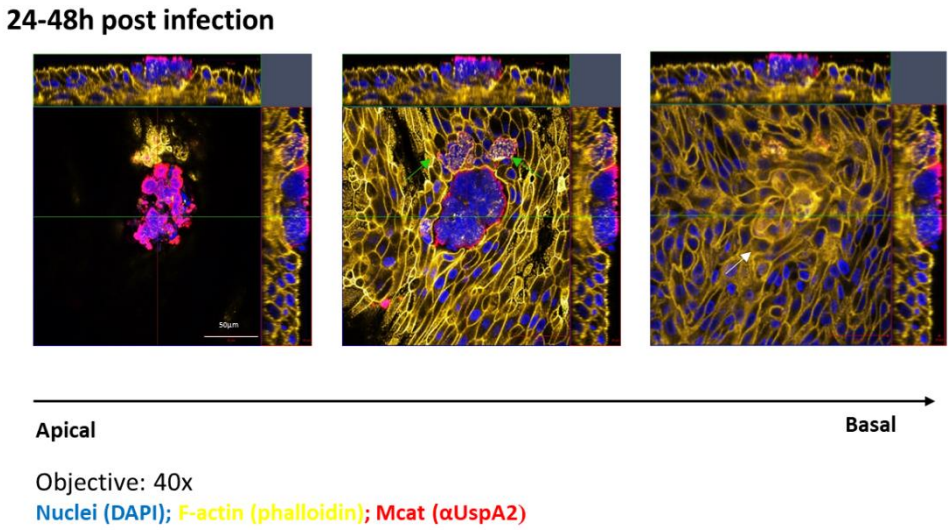


***Figure 15.*** *Progressive planes from apical to basal of respiratory tissue infected for 48h with Mcat which formed surface-associate biofilm-like structures. Regions adjacent to the nascent colony show intracellular bacteria aggregates with evident actin de-polymerization (green arrow).*

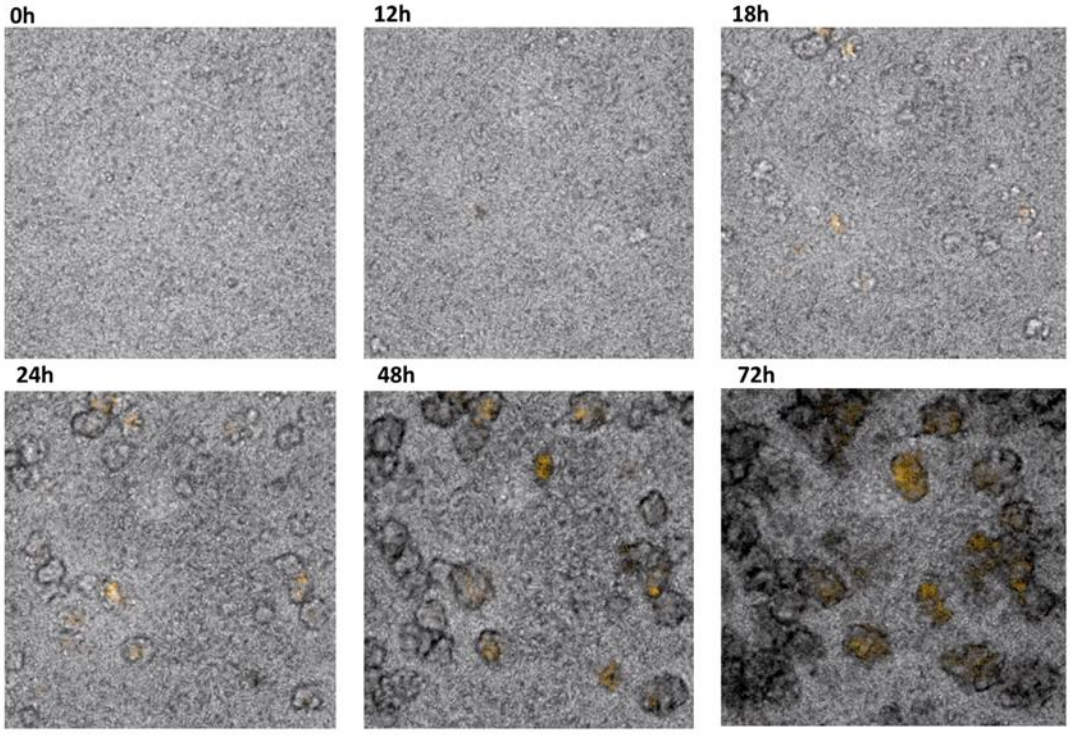


***Figure 16*** *– Time lapse of Mcat infection of MucilAir models. Mcherry fluorescent protein (highlighted in yellow) is not evenly expressed throughout the Moraxella catarrhalis population.*

## 4.5 Bacterial infection causes tissue remodeling and activation of regeneration pathways

The microscopy analysis of Mcat infection for 48 hours permitted to observe distinct pathogenic mechanisms employed by the pathogen to effectively colonize the bronchial mucosa. As a consequence of these results, several questions arose about the effects of infection on the host epithelium. Apart from the ability of Mcat to survive and grow within the infected cells, the effect on epithelial exfoliation was intriguing. Indeed despite infected cells were heavily colonized by bacteria that took control of cell structure and function, these cells were not extruded from the tissue, as normally happens in this situation[151]. Moreover, the phenomenon of cell death/tissue destruction occurs in conjunction with a clear depolymerization of actinic filaments with adjacent epithelium profoundly remodeled.

In order to further investigate this phenomenon, we established a collaboration with the 'Ultrastructure and cellular Bioimaging" group of GSK-Pharma in Stevenage to engage innovative Multiplex CellDIVE immunofluorescent microscopy for evaluation of multiple tissue markers.

Fully differentiated bronchial epithelial models were produced and infected with *Moraxella catarrhalis* at different time points (6h – 24h and 48h) in Siena, then fixed and shipped to Stevenage for microscopy analysis. Samples were then paraffin-embedded, cut in 4µm sections, baked, dewaxed, and antigens retrieved. An extended panel of cytoskeletal and junctional tissue markers was defined. Biomarker-specific antibodies were firstly tested on lung/tonsil tissue to evaluate sensitivity and specificity of staining, then selected antibody clones were used for staining and imaging of bronchial sections with Cell DIVE Leica system. Each section was stained with DAPI and imaged using all three cyanine/Alexafluor channels to provide a background "autofluorescence" reference image that was subtracted to subsequent acquisitions of experimental samples. Sections containing bacterial colonies identified with DAPI were incubated with a first set of dye-conjugated antibodies and images acquired. After this first cycle of imaging,

fluorescent probes were deactivated with hydrogen peroxide in sodium bicarbonate buffer preserving DAPI staining that was used as "control probe" for subsequent acquisitions. A second cycle of antibodies incubation followed (see Materials and methods). Each staining panel therefore contains all the biomarkers relative to the same sample during multiple staining cycles. Bacterial colonies were visible with DAPI staining since we failed to have a good signal with anti-UspA2 antibodies.

Global evaluation of cytokeratin cellular distribution (pancytokeratins antibodies, PanCKs) enabled to assess the structure of cell cytoskeleton during the formation of bacterial colonies. Bacterial distribution did not appear to be limited to a single cell but to involve also adjacent cells that looked displaced (Fig. 17, sample 1). Integrin a2, that is reported to be dynamically regulated during lung development [152,153], resulted more intensively expressed on epithelial basal cells equally in control and infected samples. The paraffin-embedding and cutting of samples sections was not always perfectly orthogonal, making difficult to correctly detect cell junctional structures such as ZO-1 and Occludin. However, in well-preserved samples (control, sample 3; infected, sample 1, and 3) it was possible to observe the apical distribution of those markers (Fig.17). Interestingly, the distribution of the newly identified club cell marker cytokeratin 17[154] (KRT 17) assumed a different distribution when in close proximity to Mcat aggregates (Fig. 18 sample 2, 3). Given the role of Club cells in tissue regeneration [129], these observations suggests a possible activation of these cells to repair the damages tissue. Moreover, also the distribution of claudin 3 (CLDN3) and claudin 7 (CLDN7) was particularly compromised during infection, as shown in figure 17 and figure 18, samples 2 and 3. In particular, CLDN7 staining was less evident in cells underlying the bacterial aggregate when compared to neighbouring cells.

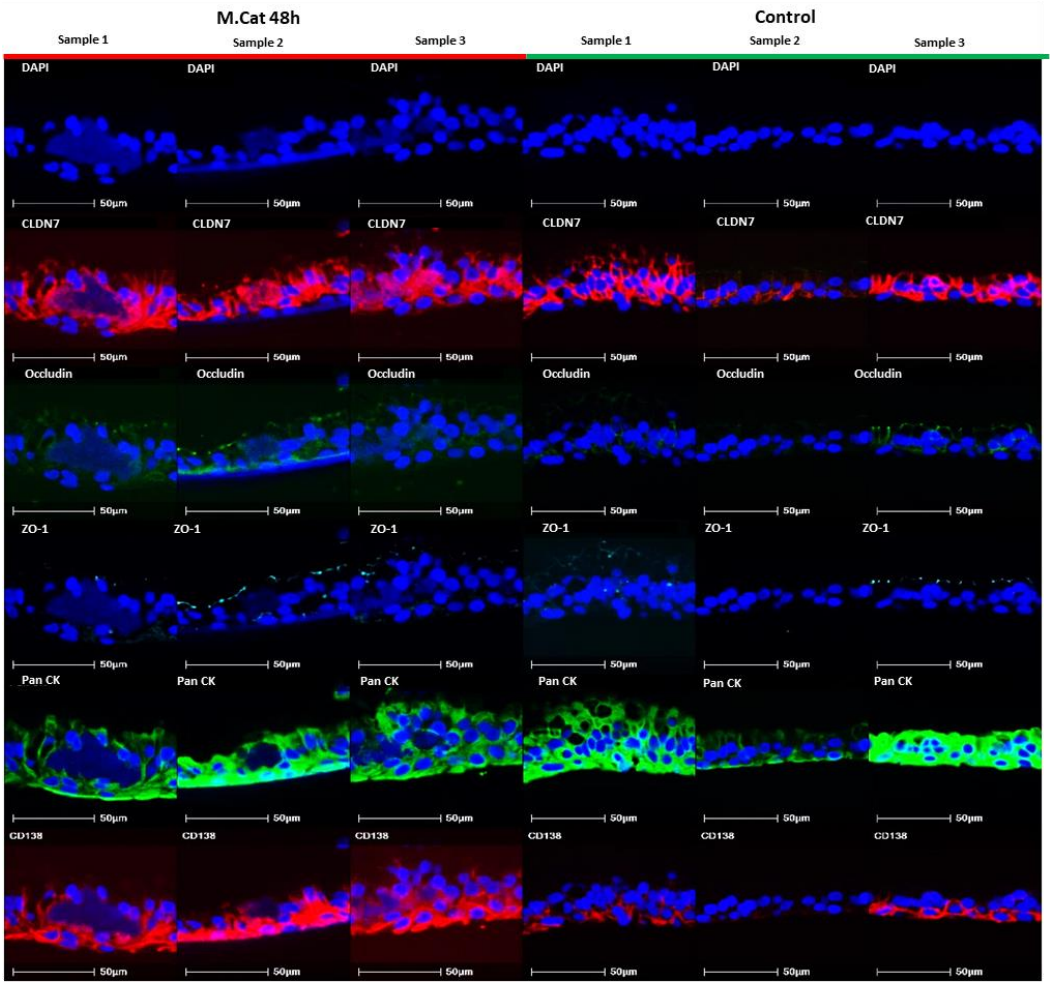


***Figure 17****. CellDive assay 1. Comparison of tissue markers distribution between three different regions of samples infected with Mcat for 48h, presenting bacterial colonies (left panel, M.cat 48h), and three controls (right panel, Control). Sections are selected and stained for DAPI (blue), CLDN7 (red), Occludin (green), ZO-1 (light blue) markers.*

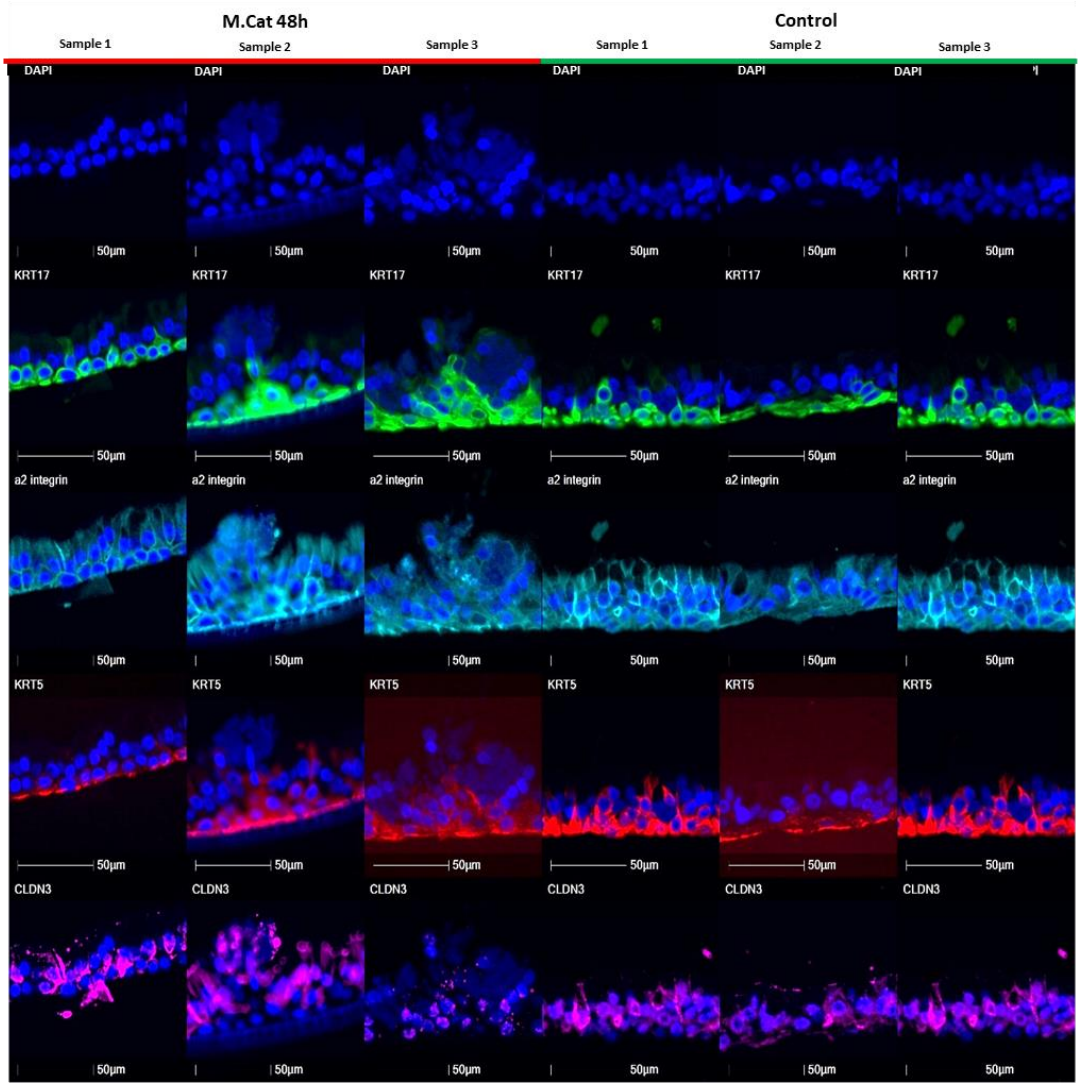


***Figure 18**. CellDive assay 2. Comparison of tissue markers distribution between three different regions of samples infected with Mcat for 48h and presenting bacterial colonies (left panel, M.cat 48h), and three controls (right panel, Control). Sections are selected and stained for DAPI (blue), KRT17 (green), a2 integrin (light blue), KRT5 (red), CLDN3 (pink) markers.*

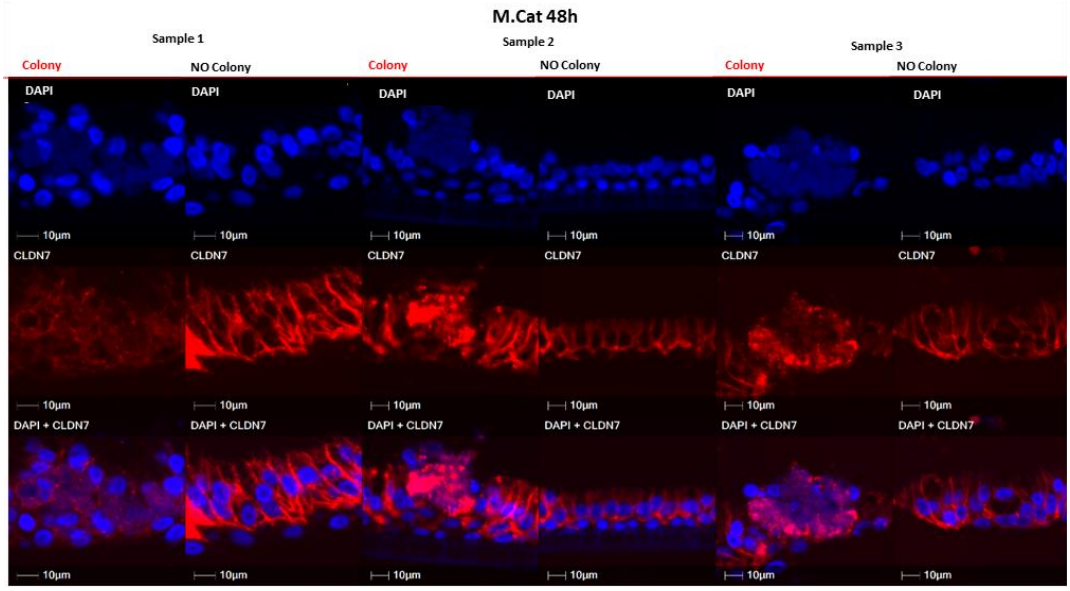


***Figure 19**. Comparison of CLDN7 (red) distribution between regions presenting and not presenting Mcat colonies within 48h infected respiratory models.*

At a closer look, images of 48h-infected samples (Fig.19) showed a consistently disruption of CLDN7, especially in regions adjacent to Mcat colonies. Representative images from different regions within the Mcat-infected samples exhibiting bacterial colonies or not, showed a different distribution of CLDN7 protein. This junctional protein seemed embedded within bacterial biomass (sample 2 and 3) while it looked deeply disrupted in proximity of intraepithelial bacteria aggregates (sample 1).

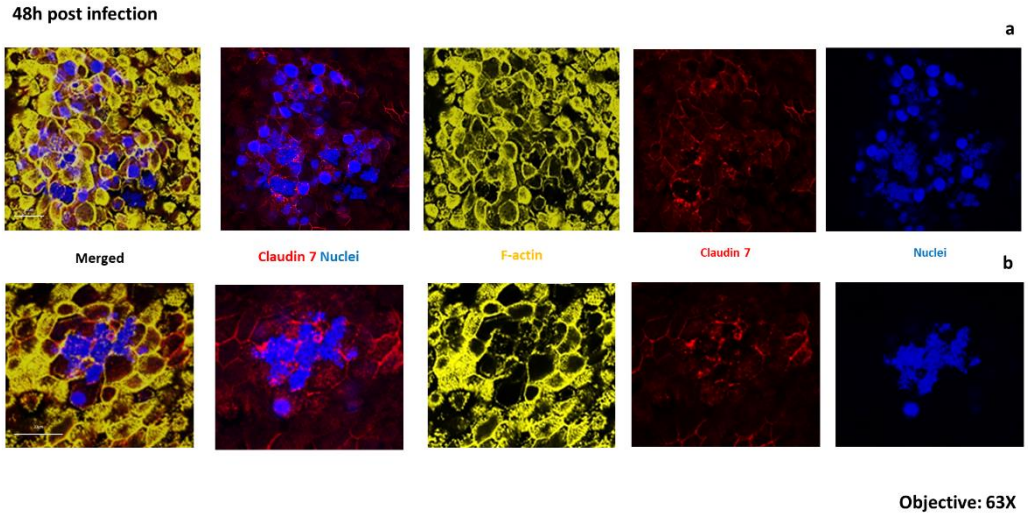


***Figure 20***. *Intraepithelial Mcat colonies formed after 48h of infection of bronchial respiratory models. Mcat colony is detectable by nuclei staining (blue), while F-actin component of cytoskeleton is marked in yellow and junctional component Claudin 7 in red.*

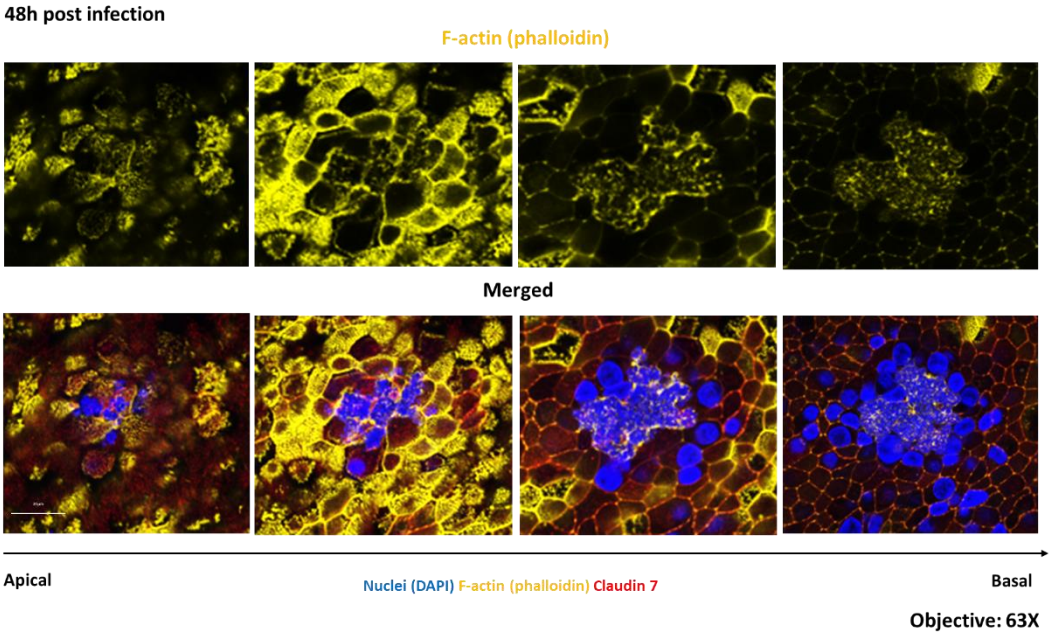


***Figure 21***. *F-actin distribution in progressive Z-plane stacks from the apical to basal side of 48h Mcat-infected samples. DAPI signal (blue) stains eukaryotic and prokaryotic nuclei, while in yellow is evident tissue distribution of F-actin and in red the junctional protein Claudin 7.*

Further investigation using confocal microscopy at higher magnifications showed a more distinct distribution of the junctional protein Claudin 7 in correspondence with the bacterial colony. This protein is particularly disaggregated at the region of epithelial tissue where the rupture and emerging of the intraepithelial colony occurred. The two images in figure 20 showed a small colony (Fig.20 b) and a larger intraepithelial bacterial colony (Fig. 20 a). In both conditions, the distribution of claudin is similarly impaired. Pictures of the junctional protein claudin 7 collected at different magnifications in place of bacterial infection of the tissue suggest a hypothetical bacterial mechanism to breach epithelial barrier, similarly to what has already been reported for the respiratory pathogens *Haemophilus influenzae* and *Streptococcus pneumonie*[155].

Since the maintenance of tissue permeability is regulated by the interaction between cell-cell junctions and cellular cytoskeletal components, we also evaluated the distribution of f-actin at bacterial colonies by progressive focal planes of Mcat-infected models (Fig.21). While pictures of the apical plane of the 48h infected tissue showed no particular signs of cytoskeleton structural alteration, subsequent basal focal planes displayed an extensive F-actin depolymerization of tissue enveloping the bacterial intraepithelial colony. It has been widely reported that pathogens can use actin-based motility system to allow bacterial invasion and cell-to-cell spread causing cytoskeleton remodeling[156–159]. Since little is known regarding Mcat strategies of spreading and persistence inside the host the analysis of infection phenotypes observed is open to speculations.

Up to now, it was observed the histologic localization of Mcat reservoir only in human pharyngeal lymphoid tissues as a hypothetical answer to host common reinfection [112]. For the first time it has been possible to recreate a similar pathogenic phenotype *in vitro* and further investigate on bacterial mechanisms used for tissue infection. The observed mislocalization of cell-cell basolateral complexes along with the presence of visible cytoskeletal rearrangement provide important information regarding the Mcat ability to manipulate epithelial components and tissue architecture to form bacterial tissue colony.

Since a wide repertoire of cytokeratins is expressed in lung depending on cell type, differentiation state and disease state, we made an exploratory analysis of differential expressed proteins in tissue infected with Moraxella for 24h and mock-infected (data not shown). High level of cytokeratin 8 and 19 were detected in control samples. Interestingly, while cytokeratin 19 levels remained constant in infected samples, overall cytokeratin 8 detection was significantly affected. Since cytokeratin 8 appears to be expressed mainly by luminal cells[160], this reduction could be associated with the extensive damage the tissue observed during the infection.

Concurrently, in order to clarify the impact of bacterial aggression on tissue TGF-β pathway was investigated. The biological functions of TGF-β are linked to ligand activation, mostly in response to environmental perturbations. Inflammatory states such as tissue damage, lead to activation of the canonical signaling pathway stimulating phosphorylation, and nuclear translocation of SMADs to regulate gene expression inducing cell proliferation. Given its crucial role in adult tissue homeostasis[161], we investigated relative levels of phosphorylated proteins involved in TGFβ pathway using a semi-quantitative sandwich-based protein array.

Briefly, five samples infected with Moraxella catarrhalis GSK415 for 48h and five mock infected controls were lysed and incubated overnight at 4°C on nitrocellulose membranes specific antibodies against selected proteins. Membranes were washed and then incubated with detection antibody cocktail for 2h at RT. After two washing, membranes were incubated with horseradish peroxidase (HRP)-labeled anti-rabbit secondary antibody at RT for 2 h. Signals were detected by Chemidoc® touch imaging system. For data analysis, numerical densitometry data were extracted, the background subtracted, and each array was normalized for its positive control signals (green squares). Finally, to compare array data, control array is defined as the "Reference Array" to which the infected arrays was normalized to.

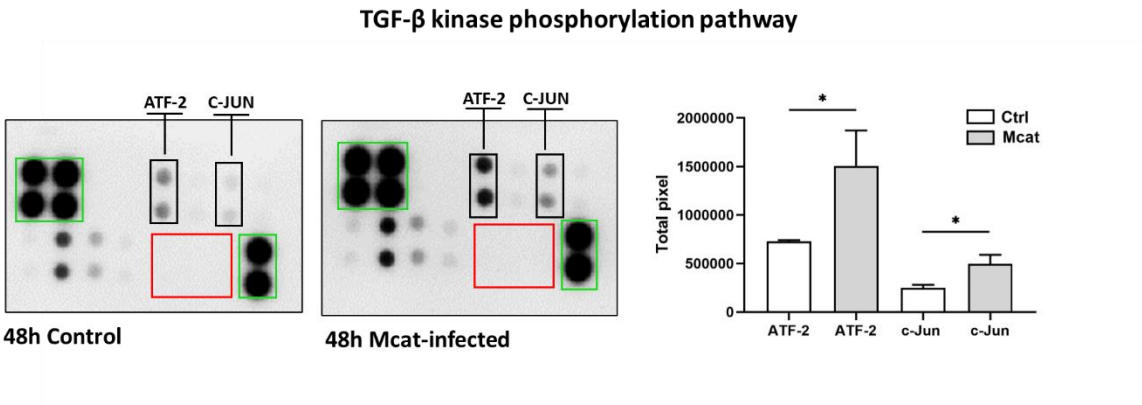


***Figure 22***. *Analysis of phospho-TGFβ array. Representative array images are shown for mock-infected and 48h infected arrays (left), and the two most phosphorylated proteins are marked in black rectangles. Positive reference spots are marked in green rectangles; area of negative control spots is marked in red rectangle. The most phosphorylated TGFβ signal molecules are displayed according total pixel intensity of phosphorylation (right). The values are represented as the mean and standard deviation calculated of three independent samples. Significance was established using two-tailed Student's t test (*P < 0.05, **P < 0.01, ***P < 0.001). All statistical analyses were performed with Prism 8.*

Results showed that two members of AP-1 proteins activating transcription factor 2 (ATF2) and transcription factor Jun (c-Jun) displayed a higher phosphorylation level (then activation) of infected samples respect to controls (Fig.22). ATF-2 is reported to be activated by many stimuli like growth factors, ultraviolet radiation and cytokines[162,163]. Growth factors and hormones are essential for the maintenance of regenerative tissues. Phosphorylation of ATF2 at amino acids Thr69 and Thr71 allows interaction with other AP1 proteins and translocation to the nucleus modulating expression of hundreds of genes[162,164,165]. The ATF2 and c-Jun dimers were reported to bind gene promoters involved in DNA repair and apoptotic signaling[162]. Moreover, activation of this transcriptional factor is related to several inflammatory diseases affecting different compartments such as obesity, hepatitis, inflammatory pain, and allergic asthma [166].

Although these are preliminary data, they support the hypothesis that bacterial infection induces an inflammatory response in the host and activates tissue regeneration later as a response to the extensive tissue damage caused by the infection.

## Conclusion and future perspectives

The present work aimed to study the pathogenesis of Moraxella catarrhalis using 3D advanced *in vitro* systems. For this purpose, we used respiratory tissue equivalents realized by co-culturing human primary epithelial cells and fibroblasts. Differentiated tissues presented a pseudostratified epithelium, consisting of different cell types and cell junctions that ensure the formation of the epithelial barrier.

In this context, we performed infection experiments with the respiratory pathogen *Moraxella catarrhalis*. The pathogen has demonstrated great adhesive capabilities to the host epithelium with tropism for ciliated cells. As previously reported, Moraxella is able to modulate gene expression to cope with hostile conditions[132]. Hence, we hypothesized that in the context of an *in vitro* colonization simulation this could have an impact on the expression of virulence factors. Indeed, results indicate that, during the initial interaction with the host, Mcat modulates its ability to interact with host cells and to incorporate metabolic factors essential for its survival. Interestingly, the concomitant presence of NTHi at these early stages causes an upregulation of genes involved in nutrient uptake, endonuclease expression, and production of the enzyme Beta-lactamase. These preliminary data obtained on a limited number of genes support the hypothesis of a possible synergistic effect existing between the two pathogens during the colonization phases of the tissue enhancing bacterial virulence and persistence strategies. As a future prospective, it would be interesting to make use of advanced high-throughput technologies for the global assessment of the bacterial and human transcriptomes and additionally investigate on the possible mechanisms employed in persistent infections by these two pathogens.

Moreover, modern microscopy technologies allowed us to deeply characterize the infection dynamics, visualizing the interactions between the pathogens and the airway epithelium. During the initial phases of Mcat infection, the pathogen is actively internalized by the host through the formation of lamellipodia, which follows the delivery of ingested bacteria to canonical pathway of phagolysosome

maturation. However, by using a yet undefined mechanism, the pathogen bypasses host clearance and duplicate intracellularly. To date, subversion mechanisms employed by Mcat to grant clearance escape are still elusive. However, many evidence support the hypothesis of a possible ROS suppression mechanism that the pathogen employs to escape intracellular killing.

Interestingly, the fact that Mcat dense intraepithelial communities resulted impermeant to immunoglobulin labeling even after cell permeabilization, suggests that immunoglobulin-mediated recognition of the pathogen *in vivo* could result limited, affecting the elimination by the immune system. One major finding of this work is the fact that the natural mechanism of cell extrusion of Mcat-infected cells seems to be blocked. In fact, infected cells are not removed from the tissue but remains firmly attached to the basal layer until growing intracellular bacterial cause its mechanical lysis. This mechanism translates into the fact that bacteria are not effectively removed from the epithelium and, on the contrary, they use the infected cell as a safe niche that shields the pathogen from the immune system. Additionally, the subsequent formation of bacterial biofilm-like structures in association with the surface of the epithelium suggests that intracellular bacterial colonies could serve as reservoir for the establishment of a more severe and chronic state of infection of the respiratory epithelium that finally ends up with epithelial-associated extracellular biofilm. The formation of Mcat bacterial colonies causes intense epithelial remodeling. Interestingly, the presence of growing intracellular bacterial colonies shows dislocation of basolateral complexes and incorporation of cell junctional complexes during bacterial spreading towards neighboring cells.

In conclusion, the employment of respiratory *in vitro* systems allowed to observe for the first time the formation of Mcat intraepithelial bacterial communities and biofilms in a context that recreates the micro-physiology of the respiratory mucosa. Mimicking such pathogenic mechanisms in a controlled environment is crucial for attempting to understand the pathogen's molecular pathways involved in pathogenesis and to identify bacterial antigens that could be used as candidates for new potential vaccines interventions.

## Acknowledgements

I would like to express my immense gratitude to my supervisor Alfredo Pezzicoli. His great expertise, guidance and patience have been crucial in supporting me through this long and puzzling journey. I would like also to thank Martina Di Fede for the precious help provided in this path with her critical feedbacks and infinite patience. I am also grateful to my PhD colleague Andrea Ariolli, the mutual support and collaboration have been fundamental in facing the challenges and misadventures of this journey. I would also thank Kevin Pete Buno and Giulia Realini for their technical assistance and precious advices. Special thanks to Marco Spinsanti, Viola Viviani, Giacomo Romagnoli e Simona Tavarini for their critical feedbacks and technical support. I would like to thank the professor Marcello Merola for this opportunity and his professional mentoring. I would express my gratitude to Isabel Delany, Silvia Rossi Paccani and Daniela Rinaudo for their critical and encouraging feedbacks on my PhD projects.

Every person I met in this experience have provided inestimable contributions to my professional and personal growth. To all, thanks.

Infine, vorrei ringraziare tutte le persone che mi hanno accompagnata e sostenuto in questo mio percorso di crescita personale. Ho deciso di catapultarmi anima e corpo in un'esperienza e in un posto del tutto nuovi. C'è voluto coraggio, e soprattutto forza, ma tutto ciò è stato possibile anche grazie all'enorme aiuto che persone lontane e vicine mi hanno dato.

Devo ringraziare la mia enorme e variegata famiglia fatta di mamma, papà, fratelli, sorelle, nipotini, zie, cugine, nonne e vecchi amici che mi hanno supportata instancabilmente in questo percorso facendomi compagnia quando la solitudine era assordante, quando la stanchezza e la paura affollavano le mie giornate. Grazie a tutti loro, per la pazienza e per l'incommensurabile affetto che instancabilmente mi avete donato. Grazie.

Grazie a tutte alle “nuove” persone che ho conosciuto lungo questo percorso, amiche, coinquiline e colleghi, il vostro aiuto, supporto, comprensione, affetto sono stati vitali e di ispirazione in questa enorme fase di crescita per me. Grazie.

Ultimo, ma imprescindibile, grazie ad Arturo che è stato tra i miei più grandi sostenitori, supportandomi quando nemmeno io ci credevo, sopportandomi nei miei periodi peggiori, e accompagnatomi anima e corpo in questa altalena di emozioni. Grazie infinitamente.

Questo periodo è stato entusiasmante, lungo, stimolante, solitario, e tutta una sequela di aggettivi che possono solo minimamente descrivere un percorso formativo come questo. È proprio vero quando si dice che bisogna andare via per scoprire sé stessi, i propri pregi, i difetti, i limiti e per riscoprire il valore gli affetti. Mi sono aperta a nuove esperienze e nuove persone. Nessuna scelta è stata più giusta.

# References


1. Iverson, E. *et al.* Leveraging 3d model systems to understand viral interactions with the respiratory mucosa. *Viruses* **12**, 1–29 (2020).

2. Hewitt, R. J. & Lloyd, C. M. Regulation of immune responses by the airway epithelial cell landscape. *Nat. Rev. Immunol.* **21**, 347–362 (2021).

3. Davis, J. D. & Wypych, T. P. Cellular and functional heterogeneity of the airway epithelium. *Mucosal Immunol.* **14**, 978–990 (2021).

4. Rock, J. R., Randell, S. H. & Hogan, B. L. M. Airway basal stem cells: A perspective on their roles in epithelial homeostasis and remodeling. *DMM Dis. Model. Mech.* **3**, 545–556 (2010).

5. Yoshida, T. & Tuder, R. M. Pathobiology of cigarette smoke-induced chronic obstructive pulmonary disease. *Physiol. Rev.* **87**, 1047–1082 (2007).

6. Ostrowski, L. E. & Bennett, W. D. Cilia and Mucociliary Clearance. *Encycl. Respir. Med. Four-Volume Set* 466–470 (2006) doi:10.1016/B0-12-370879-6/00079-X.

7. Whitsett, J. A. Airway epithelial differentiation and mucociliary clearance. *Ann. Am. Thorac. Soc.* **15**, S143–S148 (2018).

8. Plasschaert. A single cell atlas of the tracheal epitheliul reveals the CFTR-rich pulmonary ionocyte. *Physiol. Behav.* **176**, 139–148 (2019).

9. Montoro, D. T. *et al.* A revised airway epithelial hierarchy includes CFTR-expressing ionocytes. **560**, 319–324 (2019).

10. Barron, S. L., Saez, J. & Owens, R. M. In Vitro Models for Studying Respiratory Host–Pathogen Interactions. *Advanced Biology* vol. 5 (2021).

11. Hiemstra, P. S., Amatngalim, G. D., Van Der Does, A. M. & Taube, C. Antimicrobial peptides and innate lung defenses: Role in infectious and noninfectious lung diseases and therapeutic applications. *Chest* **149**, 545–551 (2016).

12. Teitelbaum, R. *et al.* The M cell as a portal of entry to the lung for the bacterial pathogen Mycobacterium tuberculosis. *Immunity* **10**, 641–650 (1999).

13. Gohy, S., Hupin, C., Ladjemi, M. Z., Hox, V. & Pilette, C. Key role of the epithelium in chronic upper airways diseases. *Clin. Exp. Allergy* **50**, 135–146 (2020).

14. González-Mariscal, L., Tapia, R. & Chamorro, D. Crosstalk of tight junction components with signaling pathways. *Biochim. Biophys. Acta - Biomembr.* **1778**, 729–756 (2008).

15. Soini, Y. Claudins in lung diseases. 1–11 (2011).

16. Mhatre V. Ho, Ji-Ann Lee, and K. C. M. & Dien et al., 2013. Desmosome dynamics in migrating epithelial cells requires the actin cytoskeleton. *Bone* **23**, 1–7 (2008).

17. Moll, R., Divo, M. & Langbein, L. The human keratins : biology and pathology. 705–733 (2008) doi:10.1007/s00418-008-0435-6.

18. González-Mariscal, L. *et al.* Tight junctions and the regulation of gene expression. *Semin. Cell Dev. Biol.* **36**, 213–223 (2014).

19. Terry, S., Nie, M., Matter, K. & Balda, M. S. Rho Signaling and Tight Junction Functions. *Physiology* **25**, 16–26 (2010).

20. Paradis, T., Bègue, H., Basmaciyan, L., Dalle, F. & Bon, F. Tight junctions as a key for pathogens invasion in intestinal epithelial cells. *Int. J. Mol. Sci.* **22**, 1–21 (2021).

21. Sharma, L., Feng, J., Britto, C. J. & Cruz, C. S. Dela. Mechanisms of Epithelial Immunity Evasion by Respiratory Bacterial Pathogens. **11**, 1–8 (2020).

22. Ioannidis, I., Ye, F., Mcnally, B. & Willette, M. Toll-Like Receptor Expression and Induction of Type I and Type III Interferons in Primary Airway Epithelial Cells. **87**, 3261–3270 (2013).

23. Pandey, S., Kawai, T. & Akira, S. Microbial sensing by toll-like receptors and intracellular nucleic acid sensors. *Cold Spring Harb. Perspect. Biol.* **7**, 1–18 (2015).

24. Jeffrey A Whitsett, T. A. Respiratory epithelial cells orchestrate pulmonary innate immunity. **16**, 27–35 (2015).

25. Kirst, M. E., Baker, D., Li, E., Abu-hasan, M. & Id, G. P. W. Upper versus lower airway microbiome and metagenome in children with cystic fibrosis and their correlation with lung inflammation. 1–15 (2019) doi:10.17026/dans-2cb-66ad.

26. Günther, J. The first line of defence : insights into mechanisms and relevance of phagocytosis in epithelial cells. 555–565 (2018).

27. Veiga, E. & Cossart, P. Listeria hijacks the clathrin-dependent endocytic machinery to invade mammalian cells. *Nat. Cell Biol.* **7**, 894–900 (2005).

28. Schlumberger, M. C. & Hardt, W. D. Salmonella type III secretion effectors: Pulling the host cell's strings. *Curr. Opin. Microbiol.* **9**, 46–54 (2006).

29. Vazquez-Torres, A. *et al.* Salmonella pathogenicity island 2-dependent evasion of the phagocyte NADPH oxidase. *Science (80-. ).* **287**, 1655–1658 (2000).

30. Czuczman, M. A. *et al.* Listeria monocytogenes exploits efferocytosis to promote cell-to-cell spread. *Nature* **509**, 230–234 (2014).

31. Heckmann, B. L., Boada-romero, E., Cunha, L. D., Magne, J. & Green, R. LC3-Associated Phagocytosis and Inflammation. **429**, 3561–3576 (2018).

32. FitzGerald, E. S., Luz, N. F. & Jamieson, A. M. Competitive Cell Death Interactions in Pulmonary Infection: Host Modulation Versus Pathogen Manipulation. *Front. Immunol.* **11**, (2020).

33. Hippenstiel, S., Opitz, B., Schmeck, B. & Suttorp, N. Lung epithelium as a sentinel and effector system in pneumonia--molecular mechanisms of pathogen recognition and signal transduction. *Respir. Res.* **7**, 97 (2006).

34. Bergsbaken, T. & Cookson, B. T. Macrophage activation redirects yersinia-infected host cell death from apoptosis to caspase-1-dependent pyroptosis. *PLoS Pathog.* **3**, e161 (2007).

35. Lamkanfi, M. & Dixit, V. M. Manipulation of host cell death pathways during

microbial infections. *Cell Host Microbe* **8**, 44–54 (2010).

36. Zitvogel, L., Kepp, O. & Kroemer, G. Decoding cell death signals in inflammation and immunity. *Cell* **140**, 798–804 (2010).

37. Ashida, H. *et al.* Cell death and infection: A double-edged sword for host and pathogen survival. *J. Cell Biol.* **195**, 931–942 (2011).

38. Gagliardi, P. A. & Primo, L. Death for life: a path from apoptotic signaling to tissue-scale effects of apoptotic epithelial extrusion. *Cell. Mol. Life Sci.* **76**, 3571–3581 (2019).

39. Elliott, M. R. & Ravichandran, K. S. Clearance of apoptotic cells: implications in health and disease. *J. Cell Biol.* **189**, 1059–1070 (2010).

40. D'Arcy, M. S. Cell death: a review of the major forms of apoptosis, necrosis and autophagy. *Cell Biol. Int.* **43**, 582–592 (2019).

41. Liu, X. & Lieberman, J. *A Mechanistic Understanding of Pyroptosis: The Fiery Death Triggered by Invasive Infection*. *Advances in Immunology* vol. 135 (Elsevier Inc., 2017).

42. Churchill, M. J., Mitchell, P. S. & Rauch, I. Epithelial Pyroptosis in Host Defense. *J. Mol. Biol.* **434**, 167278 (2022).

43. Arnoult, D., Carneiro, L., Tattoli, I. & Girardin, S. E. The role of mitochondria in cellular defense against microbial infection. *Semin. Immunol.* **21**, 223–232 (2009).

44. Rudel, T., Kepp, O. & Kozjak-Pavlovic, V. Interactions between bacterial pathogens and mitochondrial cell death pathways. *Nat. Rev. Microbiol.* **8**, 693–705 (2010).

45. Dhiman, R., Kathania, M., Raje, M. & Majumdar, S. Inhibition of bfl-1/A1 by siRNA inhibits mycobacterial growth in THP-1 cells by enhancing phagosomal acidification. *Biochim. Biophys. Acta* **1780**, 733–742 (2008).

46. Banga, S. *et al.* Legionella pneumophila inhibits macrophage apoptosis by targeting pro-death members of the Bcl2 protein family. *Proc. Natl. Acad. Sci. U. S. A.* **104**, 5121–5126 (2007).

47. Pirbhai, M., Dong, F., Zhong, Y., Pan, K. Z. & Zhong, G. The secreted protease factor CPAF is responsible for degrading pro-apoptotic BH3-only proteins in Chlamydia trachomatis-infected cells. *J. Biol. Chem.* **281**, 31495–31501 (2006).

48. Losick, V. P. & Isberg, R. R. NF-kappaB translocation prevents host cell death after low-dose challenge by Legionella pneumophila. *J. Exp. Med.* **203**, 2177–2189 (2006).

49. Ge, J. *et al.* A Legionella type IV effector activates the NF-kappaB pathway by phosphorylating the IkappaB family of inhibitors. *Proc. Natl. Acad. Sci. U. S. A.* **106**, 13725–13730 (2009).

50. Loeuillet, C. *et al.* Mycobacterium tuberculosis subverts innate immunity to evade specific effectors. *J. Immunol.* **177**, 6245–6255 (2006).

51. Behar, S. M., Divangahi, M. & Remold, H. G. Evasion of innate immunity by Mycobacterium tuberculosis: is death an exit strategy? *Nature reviews. Microbiology* vol. 8 668–674 (2010).

52. Holmes, A., Mühlen, S., Roe, A. J. & Dean, P. The EspF effector, a bacterial pathogen's Swiss army knife. *Infect. Immun.* **78**, 4445–4453 (2010).

53. Rutering, J. *et al.* Crowding induces live cell extrusion to maintain homeostatic cell numbers in epithelia. *Nature* **5**, 1–8 (2015).

54. J., G. S. A. R. Epithelial Cell Extrusion: pathways and pathologies. *Semin Cell Dev Biol* **176**, 139–148 (2018).

55. Pentecost, M., Otto, G., Theriot, J. A. & Amieva, M. R. Listeria monocytogenes invades the epithelial junctions at sites of cell extrusion. *PLoS Pathog.* **2**, 0029–0040 (2006).

56. Liesman, R. M. *et al.* RSV-encoded NS2 promotes epithelial cell shedding and distal airway obstruction. *J. Clin. Invest.* **124**, 2219–2233 (2014).

57. Muenzner, P., Rohde, M., Kneitz, S. & Hauck, C. R. CEACAM engagement by human pathogens enhances cell adhesion and counteracts bacteria-induced detachment of epithelial cells. *J. Cell Biol.* **170**, 825–836 (2005).

58. Lacroix, G. *et al.* Air-Liquid Interface in Vitro Models for Respiratory Toxicology Research: Consensus Workshop and Recommendations. *Appl. Vitr. Toxicol.* **4**, 91–106 (2018).

59. Shanks, N., Greek, R. & Greek, J. Are animal models predictive for humans? *Philos. Ethics, Humanit. Med.* **4**, 1–20 (2009).

60. Cao, X. *et al.* Invited review: human air-liquid-interface organotypic airway tissue models derived from primary tracheobronchial epithelial cells—overview and perspectives. *Vitr. Cell. Dev. Biol. - Anim.* **57**, 104–132 (2021).

61. BéruBé, K., Prytherch, Z., Job, C. & Hughes, T. Human primary bronchial lung cell constructs: The new respiratory models. *Toxicology* **278**, 311–318 (2010).

62. van der Vaart, J. & Clevers, H. Airway organoids as models of human disease. *J. Intern. Med.* **289**, 604–613 (2021).

63. Artzy-Schnirman, A., Lehr, C. M. & Sznitman, J. Advancing human in vitro pulmonary disease models in preclinical research: opportunities for lung-on-chips. *Expert Opin. Drug Deliv.* **17**, 621–625 (2020).

64. Bebök, Z., Tousson, A., Schwiebert, L. M. & Venglarik, C. J. Improved oxygenation promotes CFTR maturation and trafficking in MDCK monolayers. *Am. J. Physiol. - Cell Physiol.* **280**, 135–145 (2001).

65. Rayner, R. E., Makena, P., Prasad, G. L. & Cormet-boyaka, E. Optimization of Normal Human Bronchial Epithelial ( NHBE ) Cell 3D Cultures for in vitro Lung Model Studies. 2–11 (2019) doi:10.1038/s41598-018-36735-z.

66. Nichols, J. E. *et al.* Modeling the lung: Design and development of tissue engineered macro- and micro-physiologic lung models for research use. *Exp. Biol. Med.* **239**, 1135–1169 (2014).

67. Pezzulo, A. A. *et al.* The air-liquid interface and use of primary cell cultures are important to recapitulate the transcriptional profile of in vivo airway epithelia. *Am. J. Physiol. - Lung Cell. Mol. Physiol.* **300**, 25–31 (2011).

68. Charlson, E. S. *et al.* Topographical continuity of bacterial populations in the

healthy human respiratory tract. *Am. J. Respir. Crit. Care Med.* **184**, 957–963 (2011).

69. Lim, M. Y. *et al.* Analysis of the association between host genetics, smoking, and sputum microbiota in healthy humans. *Sci. Rep.* **6**, 1–9 (2016).

70. Earl, C. S., An, S. qi & Ryan, R. P. The changing face of asthma and its relation with microbes. *Trends Microbiol.* **23**, 408–418 (2015).

71. O'Connor, J. B. *et al.* Divergence of bacterial communities in the lower airways of CF patients in early childhood. *PLoS One* **16**, 1–17 (2021).

72. Man, W. H., De Steenhuijsen Piters, W. A. A. & Bogaert, D. The microbiota of the respiratory tract: Gatekeeper to respiratory health. *Nat. Rev. Microbiol.* **15**, 259–270 (2017).

73. Ditz, B. *et al.* Sputum microbiome profiling in COPD: Beyond singular pathogen detection. *Thorax* **75**, 338–344 (2020).

74. Ramsheh, M. Y. *et al.* Lung microbiome composition and bronchial epithelial gene expression in patients with COPD versus healthy individuals: a bacterial 16S rRNA gene sequencing and host transcriptomic analysis. *The Lancet Microbe* **2**, e300–e310 (2021).

75. Mayhew, D. *et al.* Longitudinal profiling of the lung microbiome in the AERIS study demonstrates repeatability of bacterial and eosinophilic COPD exacerbations. *Thorax* **73**, 422–430 (2018).

76. Garcha, D. S. *et al.* Changes in prevalence and load of airway bacteria using quantitative PCR in stable and exacerbated COPD. *Thorax* **67**, 1075–1080 (2012).

77. de Vries, S. P. W., Bootsma, H. J., Hays, J. P. & Hermans, P. W. M. Molecular Aspects of Moraxella catarrhalis Pathogenesis . *Microbiol. Mol. Biol. Rev.* **73**, 389–406 (2009).

78. Bernhard, S. *et al.* Outer membrane protein OlpA contributes to Moraxella catarrhalis serum resistance via interaction with factor H and the alternative pathway. *J. Infect. Dis.* **210**, 1306–1310 (2014).

79. Murphy, T. F., Brauer, A. L., Grant, B. J. B. & Sethi, S. Moraxella catarrhalis in chronic obstructive pulmonary disease: Burden of disease and immune response. *Am. J. Respir. Crit. Care Med.* **172**, 195–199 (2005).

80. Shi, W. *et al.* β-Lactamase production and antibiotic susceptibility pattern of Moraxella catarrhalis isolates collected from two county hospitals in China. *BMC Microbiol.* **18**, 1–6 (2018).

81. Blakeway, L. V., Tan, A., Peak, I. R. A. & Seib, K. L. Virulence determinants of moraxella catarrhalis: Distribution and considerations for vaccine development. *Microbiol. (United Kingdom)* **163**, 1371–1384 (2017).

82. Jaber, A. S. Moraxella catarrhalis: The virulence factor and pathogenesis strategy. *Int. J. Adv. Res. Med.* **3**, 568–576 (2021).

83. Su, Y., Singh, B. & Riesbeck, K. System To Vaccine Development. 1073–1100 (2012).

84. Ahmed, K. *et al.* Attachment of moraxella catarrhalis occurs to the positively

charged domains of pharyngeal epithelial cells. *Microb. Pathog.* **28**, 203–209 (2000).

85. Luke, N. R., Jurcisek, J. A., Bakaletz, L. O. & Campagnari, A. A. Contribution of Moraxella catarrhalis type IV pili to nasopharyngeal colonization and biofilm formation. *Infect. Immun.* **75**, 5559–5564 (2007).

86. Conners, R. *et al.* The Moraxella adhesin UspA1 binds to its human CEACAM1 receptor by a deformable trimeric coiled-coil. *EMBO J.* **27**, 1779–1789 (2008).

87. Slevogt, H. *et al.* Moraxella catarrhalis is internalized in respiratory epithelial cells by a trigger-like mechanism and initiates a TLR2- and partly NOD1-dependent inflammatory immune response. *Cell. Microbiol.* **9**, 694–707 (2007).

88. Tan, T. T., Forsgren, A. & Riesbeck, K. The Respiratory Pathogen Moraxella catarrhalis Adheres to Epithelial Cells by Interacting with Fibronectin through Ubiquitous Surface Proteins A1 and A2. **192**, 1029–1038 (2005).

89. Blom, A. M., Tan, T. T., Forsgren, A. & Riesbeck, K. Ionic Binding of C3 to the Human Pathogen Moraxella. (2018).

90. Blom, A. M., Villoutreix, B. O. & Dahlbäck, B. Complement inhibitor C4b-binding protein - Friend or foe in the innate immune system? *Mol. Immunol.* **40**, 1333–1346 (2004).

91. Meier, P. S., Troller, R., Grivea, I. N., Syrogiannopoulos, G. A. & Aebi, C. The outer membrane proteins UspA1 and UspA2 of Moraxella catarrhalis are highly conserved in nasopharyngeal isolates from young children. *Vaccine* **20**, 1754–1760 (2002).

92. Brooks, M. J. *et al.* Modular arrangement of allelic variants explains the divergence in moraxella catarrhalis uspa protein function. *Infect. Immun.* **76**, 5330–5340 (2008).

93. Ysebaert, C. *et al.* UspA2 is a cross-protective Moraxella catarrhalis vaccine antigen. *Vaccine* **39**, 5641–5649 (2021).

94. Jones, M. M. *et al.* Role of the oligopeptide permease ABC transporter of Moraxella catarrhalis in nutrient acquisition and persistence in the respiratory tract. *Infect. Immun.* **82**, 4758–4766 (2014).

95. Myers, L. E. *et al.* The transferrin binding protein B of Moraxella catarrhalis elicits bactericidal antibodies and is a potential vaccine antigen. *Infect. Immun.* **66**, 4183–4192 (1998).

96. Gray-Owen, S. D. & Schryvers, A. B. Bacterial transferrin and lactoferrin receptors. *Trends Microbiol.* **4**, 185–191 (1996).

97. Aebi, C. *et al.* Expression of the CopB outer membrane protein by Moraxella catarrhalis is regulated by iron and affects iron acquisition from transferrin and lactoferrin. *Infect. Immun.* **64**, 2024–2030 (1996).

98. Campagnari, A. A., Shanks, K. L. & Dyer, D. W. Growth of Moraxella catarrhalis with human transferrin and lactoferrin: Expression of iron-repressible proteins without siderophore production. *Infect. Immun.* **62**, 4909–4914 (1994).

99. Klingman, K. L. & Murphy, T. F. Purification and characterization of a high-molecular-weight outer membrane protein of Moraxella (Branhamella) catarrhalis.

*Infect. Immun.* **62**, 1150–1155 (1994).

100. Ruckdeschel, E. A., Kirkham, C., Lesse, A. J., Hu, Z. & Murphy, T. F. Mining the Moraxella catarrhalis genome: Identification of potential vaccine antigens expressed during human infection. *Infect. Immun.* **76**, 1599–1607 (2008).

101. Adlowitz, D. G., Hiltke, T., Lesse, A. J. & Murphy, T. F. Identification and characterization of outer membrane proteins G1a and G1b of Moraxella catarrhalis. *Vaccine* **22**, 2533–2540 (2004).

102. Easton, D. M. *et al.* Characterization of a novel porin protein from Moraxella catarrhalis and identification of an immunodominant surface loop. *J. Bacteriol.* **187**, 6528–6535 (2005).

103. Hassan, F. Molecular mechanisms of moraxella catarrhalis-induced otitis media. *Curr. Allergy Asthma Rep.* **13**, 512–517 (2013).

104. Hassan, F., Ren, D., Zhang, W., Merkel, T. J. & Gu, X. X. Moraxella catarrhalis activates murine macrophages through multiple toll like receptors and has reduced clearance in lungs from TLR4 mutant mice. *PLoS One* **7**, 1–11 (2012).

105. Peng, D., Hong, W., Choudhury, B. P., Carlson, R. W. & Gu, X. X. Moraxella catarrhalis bacterium without endotoxin, a potential vaccine candidate. *Infect. Immun.* **73**, 7569–7577 (2005).

106. Zaleski, A. *et al.* Lipooligosaccharide P(k) (Galα1-4Galβ1-4Glc) epitope of Moraxella catarrhalis is a factor in resistance to bactericidal activity mediated by normal human serum. *Infect. Immun.* **68**, 5261–5268 (2000).

107. Schaar, V., Nordström, T., Mörgelin, M. & Riesbeck, K. Moraxella catarrhalis outer membrane vesicles carry β-lactamase and promote survival of Streptococcus pneumoniae and Haemophilus influenzae by inactivating amoxicillin. *Antimicrob. Agents Chemother.* **55**, 3845–3853 (2011).

108. Johnson, D. M., Sader, H. S., Fritsche, T. R., Biedenbach, D. J. & Jones, R. N. Susceptibility trends of Haemophilus influenzae and Moraxella catarrhalis against orally administered antimicrobial agents: Five-year report from the SENTRY Antimicrobial Surveillance Program. *Diagn. Microbiol. Infect. Dis.* **47**, 373–376 (2003).

109. Tan, T. T., Forsgren, A. & Riesbeck, K. The respiratory pathogen Moraxella catarrhalis binds to laminin via ubiquitous surface proteins A1 and A2. *J. Infect. Dis.* **194**, 493–497 (2006).

110. Sethi, S. & Murphy, T. F. Infection in the Pathogenesis and Course of Chronic Obstructive Pulmonary Disease. *N. Engl. J. Med.* **359**, 2355–2365 (2008).

111. Spaniol, V., Heiniger, N., Troller, R. & Aebi, C. Outer membrane protein UspA1 and lipooligosaccharide are involved in invasion of human epithelial cells by Moraxella catarrhalis. **10**, 3–11 (2008).

112. Heiniger, N., Spaniol, V., Troller, R., Vischer, M. & Aebi, C. A reservoir of Moraxella catarrhalis in human pharyngeal lymphoid tissue. *J. Infect. Dis.* **196**, 1080–1087 (2007).

113. Pearson, M. M., Laurence, C. A., Guinn, S. E. & Hansen, E. J. Biofilm formation by Moraxella catarrhalis in vitro: Roles of the UspA1 adhesin and the Hag hemagglutinin. *Infect. Immun.* **74**, 1588–1596 (2006).

114. Hall-Stoodley, L. *et al.* Direct detection of bacterial biofilms on the middle-ear mucosa of children with chronic otitis media. *Jama* **296**, 202–211 (2006).

115. Dos Santos, A. L. S. *et al.* What are the advantages of living in a community? A microbial biofilm perspective! *Mem. Inst. Oswaldo Cruz* **113**, 1–7 (2018).

116. Verhaegh, S. J. *et al.* Age-related genotypic and phenotypic differences in Moraxella catarrhalis isolates from children and adults presenting with respiratory disease in 2001-2002. *Microbiology* **154**, 1178–1184 (2008).

117. Tan, A. *et al.* Moraxella catarrhalis NucM is an entry nuclease involved in extracellular DNA and RNA degradation , cell competence and biofilm scaffolding Institute for Glycomics , Griffith University , Gold Coast , Queensland , 4215 , Australia Institute of Health and . 1–6.

118. Slevogt, H. *et al.* CEACAM1 inhibits Toll-like receptor 2-triggered antibacterial responses of human pulmonary epithelial cells. *Nat. Immunol.* **9**, 1270–1278 (2008).

119. Hoopman, T. C. *et al.* Identification of Gene Products Involved in the Oxidative Stress Response of Moraxella catarrhalis □ †. **79**, 745–755 (2011).

120. Nicchi, S. *et al.* Moraxella catarrhalis evades neutrophil oxidative stress responses providing a safer niche for nontypeable Haemophilus influenzae. *ISCIENCE* **25**, 103931 (2022).

121. Mocca, B. & Wang, W. Bacterium-generated nitric oxide hijacks host tumor necrosis factor alpha signaling and modulates the host cell cycle in vitro. *J. Bacteriol.* **194**, 4059–4068 (2012).

122. Yonker, L. M. *et al.* Development of a Primary Human Co-Culture Model of Inflamed Airway Mucosa. *Sci. Rep.* **7**, 1–12 (2017).

123. Malinowski, K., Pullis, C., Raisbeck, A. P. & Rapaport, F. T. Modulation of human lymphocyte marker expression by γ irradiation and mitomycin C. *Cell. Immunol.* **143**, 368–377 (1992).

124. Mutagenesis, S., Klock, H. E. & Lesley, S. A. Chapter 6 The Polymerase Incomplete Primer Extension ( PIPE ) Method Applied to High-Throughput Cloning. **498**, 91–103.

125. Tan, A. *et al.* Moraxella catarrhalis NucM is an entry nuclease involved in extracellular DNA and RNA degradation , cell competence and biofilm scaffolding. *Sci. Rep.* 1–14 (2019) doi:10.1038/s41598-019-39374-0.

126. Livak, K. J. & Schmittgen, T. D. Analysis of relative gene expression data using real-time quantitative PCR and the 2-ΔΔCT method. *Methods* **25**, 402–408 (2001).

127. Pageau, S. C., Sazonova, O. V., Wong, J. Y., Soto, A. M. & Sonnenschein, C. The effect of stromal components on the modulation of the phenotype of human bronchial epithelial cells in 3D culture. *Biomaterials* **32**, 7169–7180 (2011).

128. Steinke, M. *et al.* An engineered 3D human airway mucosa model based on an SIS scaffold. *Biomaterials* **35**, 7355–7362 (2014).

129. Hong, K. U., Reynolds, S. D., Giangreco, A., Hurley, C. M. & Stripp, B. R. Clara Cell Secretory Protein – Expressing Cells of the Airway Neuroepithelial Body Microenvironment Include a Label-Retaining Subset and Are Critical for

Epithelial Renewal after Progenitor Cell Depletion.

130. Balder, R., Krunkosky, T. M., Nguyen, C. Q., Feezel, L. & Lafontaine, E. R. Hag mediates adherence of Moraxella catarrhalis to ciliated human airway cells. *Infect. Immun.* **77**, 4597–4608 (2009).

131. Vries, S. P. W. De, Eleveld, M. J., Hermans, P. W. M. & Bootsma, H. J. Characterization of the Molecular Interplay between Moraxella catarrhalis and Human Respiratory Tract Epithelial Cells. **8**, 1–10 (2013).

132. Spaniol, V., Troller, R. & Aebi, C. Physiologic cold shock increases adherence of moraxella catarrhalis to and secretion of interleukin 8 in human upper respiratory tract epithelial cells. *J. Infect. Dis.* **200**, 1593–1601 (2009).

133. Tan, A. *et al.* Moraxella catarrhalis phase-variable loci show differences in expression during conditions relevant to disease. *PLoS One* **15**, 1–18 (2020).

134. Hoopman, T. C. *et al.* Use of the chinchilla model for nasopharyngeal colonization to study gene expression by Moraxella catarrhalis. *Infect. Immun.* **80**, 982–995 (2012).

135. Pogoutse, A. K. & Moraes, T. F. Iron acquisition through the bacterial transferrin receptor Iron acquisition through the bacterial transferrin receptor. **9238**, (2017).

136. Perez, A. C. & Murphy, T. F. Potential impact of a Moraxella catarrhalis vaccine in COPD. *Vaccine* **37**, 5551–5558 (2019).

137. Bair, K. L. & Campagnari, A. A. Moraxella catarrhalis Promotes Stable Polymicrobial Biofilms With the Major Otopathogens. *Front. Microbiol.* **10**, 1–9 (2020).

138. Thuan, T. T., Mörgelin, M., Forsgren, A. & Riesbeck, K. Haemophilus influenzae survival during complement-mediated attacks is promoted by Moraxella catarrhalis outer membrane vesicles. *J. Infect. Dis.* **195**, 1661–1670 (2007).

139. Armbruster, C. E. *et al.* Indirect pathogenicity of Haemophilus influenzae and Moraxella catarrhalis in Polymicrobial Otitis media occurs via interspecies quorum signaling. *MBio* **1**, 1–9 (2010).

140. Mix, A. K., Goob, G., Sontowski, E. & Hauck, C. R. Microscale communication between bacterial pathogens and the host epithelium. *Genes Immun.* **22**, 247–254 (2021).

141. Bierne, H. *et al.* Article A role for cofilin and LIM kinase in Listeria -induced phagocytosis. **42**, 101–112 (2000).

142. Rolhion, N. & Cossart, P. How the study of Listeria monocytogenes has led to new concepts in biology . To cite this version : HAL Id : pasteur-01574990. 0–35 (2017).

143. Sousa, S. *et al.* Src , cortactin and Arp2 / 3 complex are required for E-cadherin-mediated internalization of Listeria into cells. **9**, 2629–2643 (2007).

144. Valencia-gallardo, C. M., Carayol, N. & Nhieu, G. T. Van. Microreview Cytoskeletal mechanics during Shigella invasion and dissemination in epithelial cells. **17**, 174–182 (2015).

145. Krendel, M. & Gauthier, N. C. Building the phagocytic cup on an actin scaffold.

*Curr. Opin. Cell Biol.* **77**, 102112 (2022).

146. Wang, D. *et al.* Capping protein regulates endosomal trafficking by controlling f-actin density around endocytic vesicles and recruiting rab5 effectors. *Elife* **10**, 1–25 (2021).

147. Liu, Y. li *et al.* Correlation of Moraxella catarrhalis macrolide susceptibility with the ability to adhere and invade human respiratory epithelial cells. *Emerg. Microbes Infect.* **11**, 2055–2068 (2022).

148. Ohsawa S., Vaughen J., I. T. Cell Extrusion: A stress-responsive force for good or evil in epithelila homeostasis. **44**, 284–296 (2018).

149. N'Guessan, P. D. *et al.* The Moraxella catarrhalis-induced pro-inflammatory immune response is enhanced by the activation of the epidermal growth factor receptor in human pulmonary epithelial cells. *Biochem. Biophys. Res. Commun.* **450**, 1038–1044 (2014).

150. Thornton, R. B. *et al.* Multi-species bacterial biofilm and intracellular infection in otitis media. *BMC Pediatr.* **11**, (2011).

151. Sellin, M. E. *et al.* Epithelium-intrinsic NAIP/NLRC4 inflammasome drives infected enterocyte expulsion to restrict salmonella replication in the intestinal mucosa. *Cell Host Microbe* **16**, 237–248 (2014).

152. Kern, A. & Marcantonio, E. E. Role of the I-domain in collagen binding specificity and activation of the integrins α1β1 and α2β1. *J. Cell. Physiol.* **176**, 634–641 (1998).

153. Sheppard, D. Functions of pulmonary epithelial integrins: From development to disease. *Physiol. Rev.* **83**, 673–686 (2003).

154. Ruiz, S. *et al. Novel dynamics of human mucociliary differentiation revealed by single-cell RNA sequencing of nasal epithelial cultures*. (2019). doi:10.1242/dev.177428.

155. Clarke, T. B., Francella, N., Huegel, A. & Weiser, J. N. Translocation across the Epithelium. **9**, 404–414 (2015).

156. Pizarro-Cerdá, J. & Cossart, P. Listeria monocytogenes: cell biology of invasion and intracellular growth. *Microbiol. Spectr.* **6**, (2018).

157. Mittal, R. *et al.* In vitro interaction of Pseudomonas aeruginosa with human middle ear epithelial cells. *PLoS One* **9**, e91885 (2014).

158. Haglund, C. M. & Welch, M. D. Pathogens and polymers: microbe-host interactions illuminate the cytoskeleton. *J. Cell Biol.* **195**, 7–17 (2011).

159. Carabeo, R. Bacterial subversion of host actin dynamics at the plasma membrane. *Cell. Microbiol.* **13**, 1460–1469 (2011).

160. Rock, J. R. *et al.* Basal cells as stem cells of the mouse trachea and human airway epithelium. *Proc. Natl. Acad. Sci. U. S. A.* **106**, 12771–12775 (2009).

161. Hao, Y., Baker, D. & Dijke, P. Ten. TGF-β-mediated epithelial-mesenchymal transition and cancer metastasis. *Int. J. Mol. Sci.* **20**, (2019).

162. Hayakawa, J. *et al.* Identification of promoters bound by c-Jun/ATF2 during rapid large-scale gene activation following genotoxic stress. *Mol. Cell* **16**, 521–535

(2004).

163. Watson, G., Ronai, Z. & Lau, E. Factors in Biology and Disease. 347–357 (2018) doi:10.1016/j.phrs.2017.02.004.ATF2.

164. Lau, E. & Ronai, Z. A. ATF2 - at the crossroad of nuclear and cytosolic functions. *J. Cell Sci.* **125**, 2815–2824 (2012).

165. Bailey, J. & Europe-Finner, G. N. Identification of human myometrial target genes of the c-Jun NH2-terminal kinase (JNK) pathway: the role of activating transcription factor 2 (ATF2) and a novel spliced isoform ATF2-small. *J. Mol. Endocrinol.* **34**, 19–35 (2005).

166. Yu, T. *et al.* The regulatory role of activating transcription factor 2 in inflammation. *Mediators Inflamm.* **2014**, (2014).